Published OnlineFirst January 18, 2011; DOI:10.1158/0008-5472.CAN-10-2164

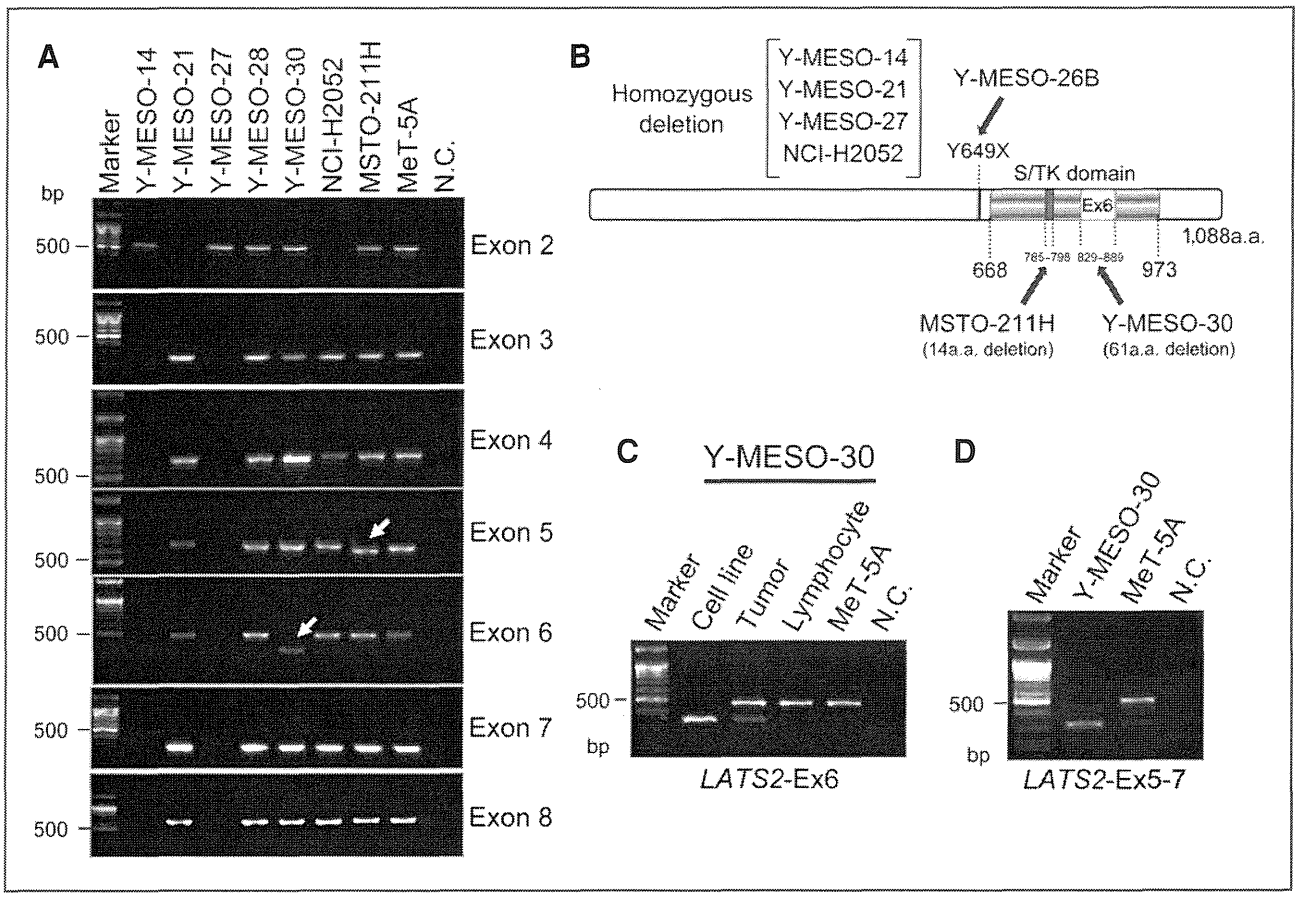

Figure 2. Genetic inactivations of *LATS2* in MM cells. A, genomic PCR analysis detected homozygous deletion in Y-MESO-14, -21, -27, and NCI-H2052, and shorter fragments in Y-MESO-30 and MSTO-211H cell lines (arrows). B, a diagram of 7 *LATS2* inactivating mutations in MM cell lines. C, genomic PCR analysis detected a shorter product by 125 bp in the Y-MESO-30 cell line and its corresponding tumor but not in lymphocytes. This deletion disrupted the donor site of the exon 6 boundary (14 bp in exon 6 and 111 bp in intron 6). D, RT-PCR analysis covering exon 5–7 detected a shorter fragment skipping exon 6, which caused the deletion of 61 amino acids coded by 183 nucleotides of exon 6.

LATS2 acts as a growth suppressor in MM cells

To determine whether the regulation of YAP by cell density was abrogated in MM cells, we then analyzed the change of cellular localization of YAP with immunocytochemistry. All 3 MM cell lines with *LATS2* mutation showed nuclear accumulation of YAP even at high cell density, whereas MeT-5A, immortalized, nonmalignant mesothelial cells, showed nuclear accumulation at low cell density but presented cytoplasmic translocation at high cell density (Fig. 4C). As expected, Western blot analysis showed that the subcellular localization change of YAP in MeT-5A according to high cell density was accompanied with a significant increase in phosphorylated YAP (Fig. 4D). In contrast, the basal levels of YAP phosphorylation in MM cells were low and there was only a modest increase in YAP phosphorylation levels (Fig. 4D).

To determine whether LATS2 has a growth-suppressive activity, we transduced the both wild-type and mutant *LATS2* constructs in MM cells. Transduction of the wild-type, but not the mutant, *LATS2* inhibited cell proliferation of MM cells with *LATS2* mutation, indicating that LATS2 acts as a growth suppressor in MM cells *in vitro* (Fig. 5A and Supplementary Fig. 2A). We also carried out anchorage-independent colony formation and Transwell migration assays and found that *LATS2* transduction in MM cell lines with *LATS2* mutation inhibited both activities in these cell lines (Fig. 5B and C and Supplementary Fig. 2B).

Finally, we carried out a knockdown experiment of LATS2 in MeT-5A cells to determine whether silencing of LATS2 promotes cell growth of nonmalignant mesothelial cells. LATS2 knockdown significantly decreased YAP phosphorylation status and slightly increased YAP protein level (Supplementary Fig. 3A). We found that silencing of LATS2 increased the cell proliferation of MeT-5A cells under low serum condition (Supplementary Fig. 3B and C), but the colony formation in soft agar was not enhanced (data not shown). These results suggested that LATS2 was involved in the regulation of cell proliferation of nonmalignant mesothelial cells as well as MM cells.

Immunohistochemical analysis of LATS2 and YAP in primary MMs

To determine whether immunostaining can be useful to detect LATS2 inactivation status in MMs, we carried out immunohistochemical analysis with anti-LATS2 antibody

Published OnlineFirst January 18, 2011; DOI:10.1158/0008-5472.CAN-10-2164

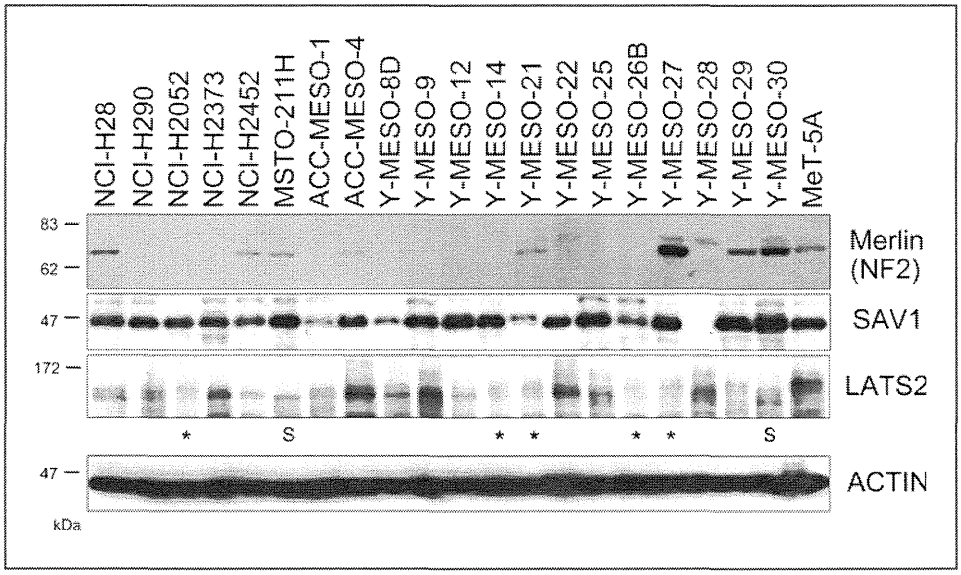

Figure 3. Western blot analysis of Merlin, SAV1, and LATS2. LATS2 protein was undetectable in 5 cell lines harboring a homozygous deletion or a premature termination, although faint nonspecific bands with slower mobility than the wild-type LATS2 were observed (indicated by asterisks). Aberrant short LATS2 proteins were detected in MSTO-211H and Y-MESO-30 (indicated by "S"). Expression of β-actin was used as the control.

(Fig. 6). The 2 MM tumors with homozygous deletion detected by array CGH analysis showed negative or only weak staining of LATS2, suggesting that weak (1+) signals might be caused by nonspecific staining. Among 45 cases, 2 showed negative and 11 showed weak staining of LATS2, whereas 32 had moderate or strong staining of LATS2, suggesting that 13 (29%) of 45 primary MMs had down-regulation of LATS2.

We also carried out immunohistochemical analysis to determine how frequently primary MMs show YAP activation (Fig. 6). Among 45 cases, 36 showed positive staining for YAP and 33 tumors showed stronger or equal staining of YAP in the nucleus

Table 1. Inactivation of *NF2*, *LATS2*, and *SAV1* in MM cell lines

Cell line	*NF2*[a]	*LATS2*	*SAV1*
NCI-H290	HD	+	+
NCI-H2373	HD	+	+
ACC-MESO-1	Q389X	+	+
Y-MESO-9	NM_000268:c.527_528del2	+	+
Y-MESO-12	HD	+	+
Y-MESO-22	HD	+	+
Y-MESO-25	NM_000268:c.532_571del40	+	+
Y-MESO-14	Q196X	HD	+
Y-MESO-26B	HD	Y649X	+
NCI-H2052	R341X	HD	+
Y-MESO-21	+	HD	+
Y-MESO-27	+	HD	+
Y-MESO-30	+	NM_014572:c.2652_2665+111del125	+
MSTO-211H	+	NM_014572:c.2355_2396del42	+
Y-MESO-28	–[b]	+	HD
Y-MESO-8D	–[b]	+	+
NCI-H28	+	+	+
NCI-H2452	+	+	+
ACC-MESO-4	+	+	+
Y-MESO-29	+	+	+

Abbreviation: HD, homozygous deletion.

[a]Mutation status of *NF2* in 9 cell lines (ACC-MESO-1, -4, Y-MESO-8D, NCI-H28, -H290, -H2052, -H2373, -H2452, and MSTO-211H) was previously described (11, 29, 30), and the one in the other 11 cell lines was analyzed in the present study.

[b]Silenced expression.

Published OnlineFirst January 18, 2011; DOI:10.1158/0008-5472.CAN-10-2164

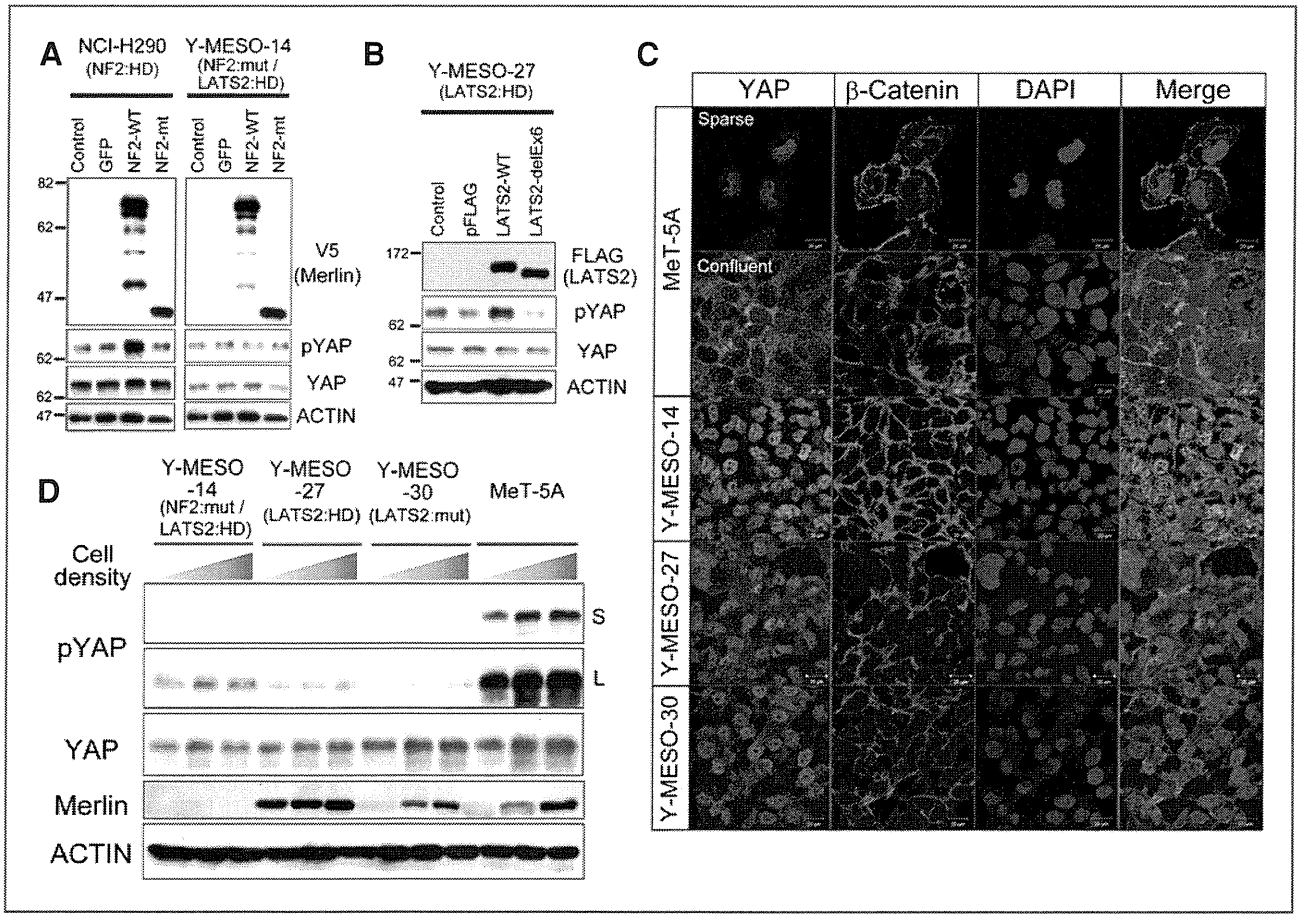

Figure 4. Inactivation of the Merlin-Hippo signaling pathway in MM cells. A, wild-type *NF2* (NF2-WT), but not truncated *NF2* (NF2-mt), induced phosphorylation of YAP in NCI-H290 cells with *NF2* homozygous deletion (HD). In contrast, wild-type *NF2* did not induce phosphorylation of YAP in Y-MESO-14 cells with both *NF2* mutation and *LATS2* HD. B, wild-type *LATS2*, but not mutant *LATS2* with exon 6-deletion (LATS2-delEx6), induced phosphorylation of YAP in Y-MESO-27 cells with *LATS2* HD, indicating that this aberrant form detected in Y-MESO-30 was kinase dead. C, MeT-5A showed YAP translocation in the cytoplasm at high cell density, whereas YAP in MM cells remained in the nucleus at high cell density. D, YAP phosphorylation according to the increasing cell density was induced in MeT-5A, whereas the basal levels of phospho-YAP (pYAP) were low at low cell density in the 3 MM cell lines. Only a modest increase in YAP phosphorylation was observed according to the higher cell density. S, short exposure; L, long exposure.

than in cytoplasm, indicating constitutive YAP activation in more than 70% of primary MMs (Supplementary Table 1).

We finally studied the relation of LATS2 expression with YAP activation status (Supplementary Table 2). Among 13 tumors with negative or weak LATS2 expression, 11 had stronger or equal staining of YAP in the nucleus, suggesting that negative or weak LATS2 may be an indicator of YAP activation.

Discussion

In the present study, we showed that *LATS2* was genetically inactivated in 7 of 20 MM cell lines and 3 of 25 primary tumors. We found that MM cells with *LATS2* mutation showed constitutive activation of YAP with underphosphorylation, regardless of high cell density, whereas YAP in nonmalignant mesothelial cells was phosphorylated and inactivated at high cell density. We further showed that transduction of *LATS2* into MM cells with *LATS2* mutation induced phosphorylation of YAP, which resulted in suppression of MM cell proliferation and anchorage-independent growth. Our study indicates that *LATS2* may be a TSG in MM cells.

Merlin is a membrane–cytoskeleton-associated protein with an FERM (Four-point-one, Ezrin, Radixin, and Moesin) domain, and is known to interact with 34 proteins, including CD44, ERM (ezrin radixin moesin) proteins, and PAK1 (p21-activated kinase 1; ref. 34). The prevalence of *NF2* mutations in sporadic tumors, especially schwannomas, meningiomas, and MMs, suggest that Merlin has a relatively broad tumor suppressor function (35, 36). Merlin and the ERM proteins have been suggested to function to both stabilize the membrane–cytoskeleton interface and to organize the distribution of, and signaling by, membrane receptors (37). Merlin exerts inhibitory effects on multiple mitogenic signaling pathways such as RAS-ERK, PI3K-AKT, and mTOR. A recent study also indicated that a closed, growth-inhibitory form of Merlin accumulates in

Published OnlineFirst January 18, 2011; DOI:10.1158/0008-5472.CAN-10-2164

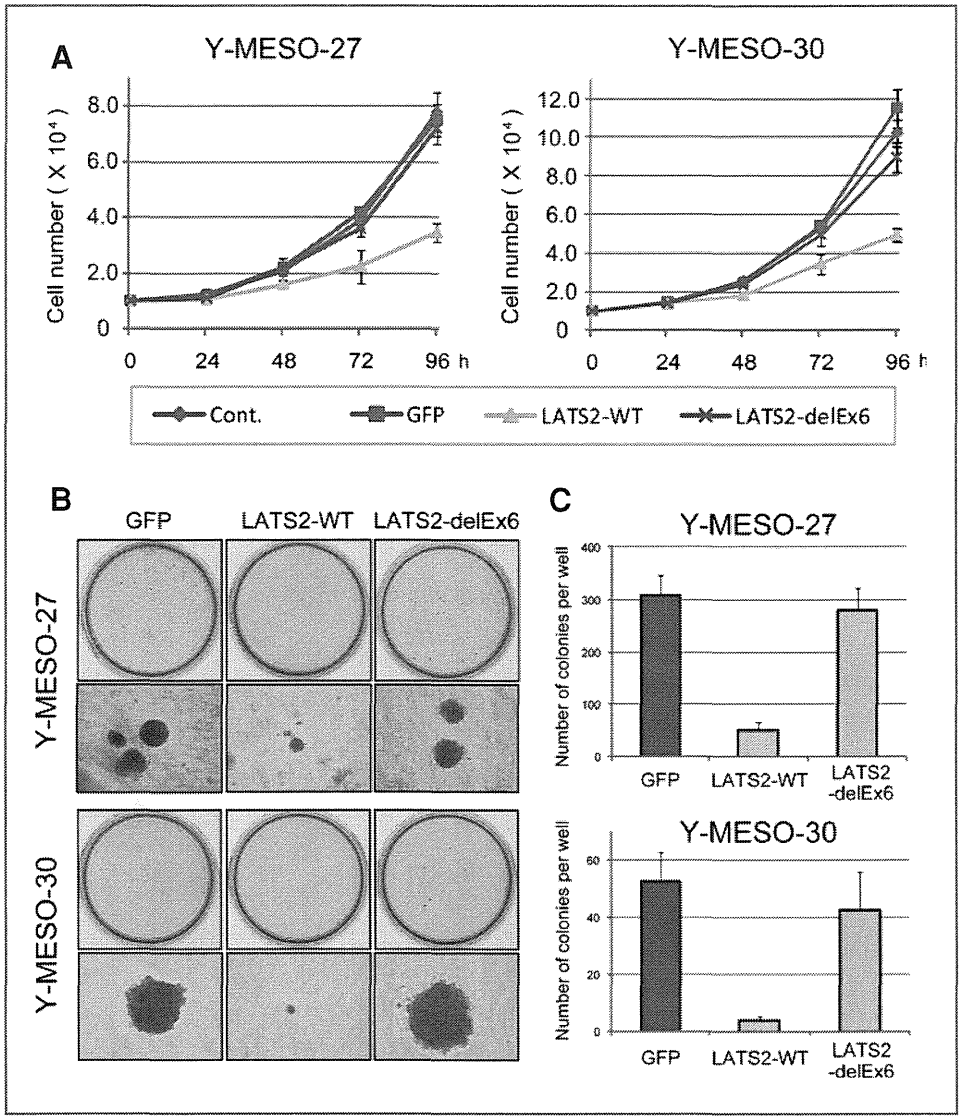

Figure 5. *LATS2* acts as a TSG in MM cells. A, inhibition of cell proliferation of Y-MESO-27 and Y-MESO-30 cells by re-expression of *LATS2*. Cells were transduced with wild-type *LATS2* (LATS2-WT), mutant *LATS2* (LATS2-delEx6), or GFP viruses (GFP), or uninfected (Cont.). Cell numbers were counted every 24 hours. Points, mean; bars, SD. B, re-expression of LATS2-WT in MM cell lines suppressed anchorage-independent colony formation. Representative results of the Y-MESO-27 and Y-MESO-30 cell lines are shown (top) with higher magnifications of their representative colonies (bottom). C, the numbers of colonies in the triplicate experiments are presented. Columns, mean; bars, SD.

the nucleus, binds to the E3 ubiquitin ligase $CRL4^{DCAF1}$, and suppresses its activity (38). In addition to these pathways, the Hippo pathway is thought to be one of the downstream signaling pathways of Merlin, which is regulated via signaling with cell–cell adhesion, cell–cellular matrix, or other cell membrane receptors with binding of extracellular ligands (21).

Dysregulation of the Hippo pathway causes an increase in organ size both in *Drosophila* and in mammalians (22). The recent findings indicated that a variety of human malignancies, such as homozygous deletion of *SAV1* in renal cancer cell lines (33) and hypermethylation of *MST* in soft tissue sarcoma (39), have alterations in each component. Overexpression of *YAP* was reported in hepatocellular carcinomas (40) and colonic and lung adenocarcinomas (41). In our previous study, we also reported *YAP* amplification in a subset of MM cells (28). Regarding *LATS2*, downregulation of *LATS2* was reported to be correlated with poor prognosis of leukemia (42) and missense mutation was also reported in lung cancer (43). However, null status of *LATS2* such as by homozygous deletion or nonsense mutation was not reported in these malignancies.

Why only 40% to 50% of MMs have *NF2* mutation and the rest do not has been a long-standing enigma. The representative hypotheses for them are that MM tumors without an *NF2* mutation may not express functional Merlin, or that the other molecules of Merlin-associated signaling cascades are altered. Supporting the former hypothesis, one study indicated that Merlin was phosphorylated on Ser518 if present and functionally inactivated in MM cells with elevated CPI-17, a cellular inhibitor of myosin phosphatase MYPT1-PP1δ (19), and the other showed that upregulation of microRNAs, such as hsa-miR-885-3p, might target *NF2* (20). Meanwhile, our data may explain the latter hypothesis, indicating that one of the major downstream pathways of Merlin can be inactivated with an *LATS2* or *SAV1* mutation. We think of the idea that *LATS2* is a TSG of MM is supported by the evidence that the mutation frequency of *LATS* was in 22% (10 of 45 MMs including 20 cell lines and 25 primary tumors), and that the

Published OnlineFirst January 18, 2011; DOI:10.1158/0008-5472.CAN-10-2164

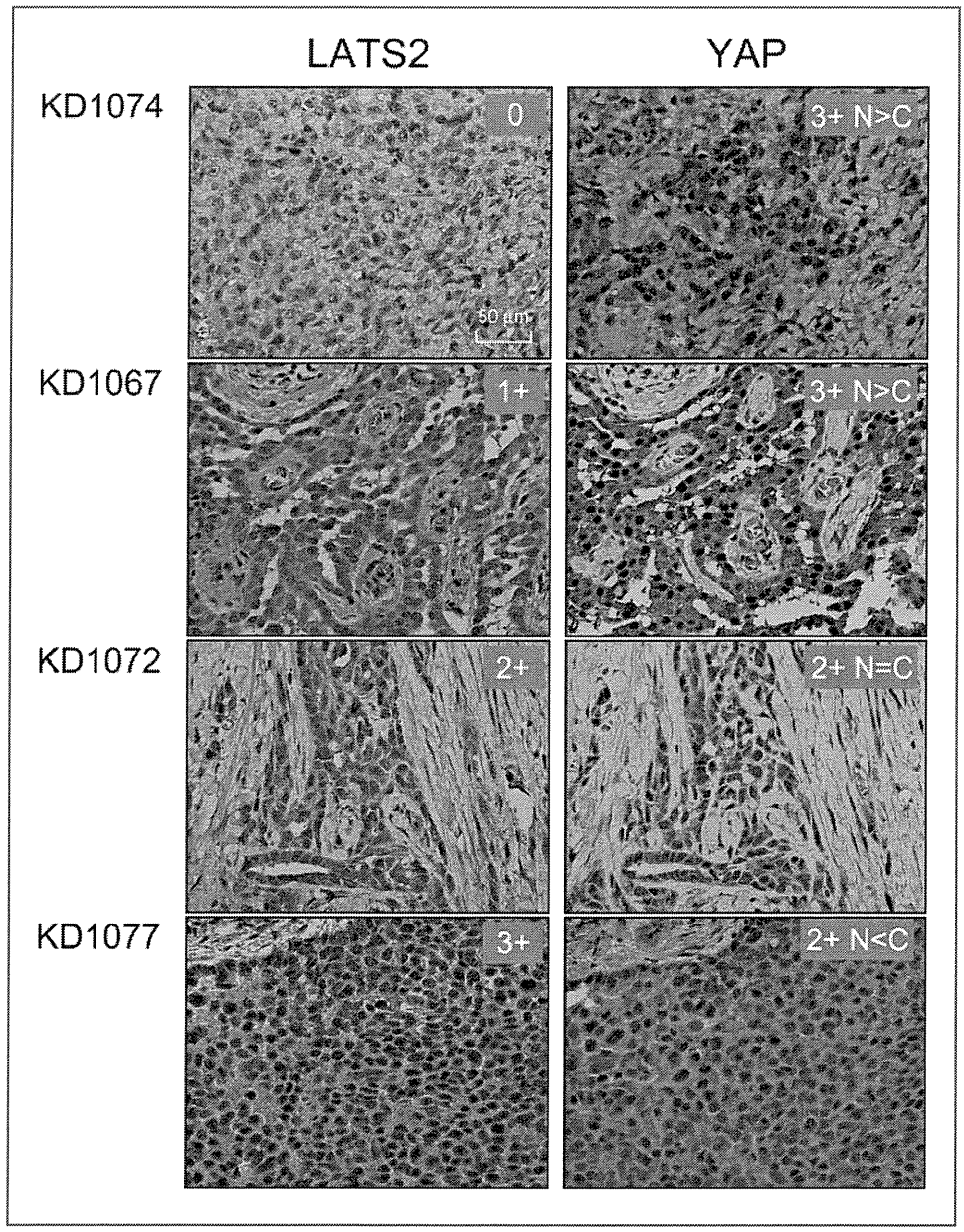

Figure 6. Immunohistochemical analyses of LATS2 and YAP in 45 primary MMs. Representative cases of LATS2 and YAP staining are presented. Case KD1074 with *LATS2* homozygous deletion and case KD1067 with *LATS2* deletion showed negative (0) and weak (1+) LATS2 staining, respectively. Both cases showed stronger staining of YAP in the nucleus. Meanwhile, cases KD1072 and KD1077 without *LATS2* deletion showed moderate (2+) and strong (3+) LATS2 staining, respectively. N, nucleus; C, cytoplasm.

characteristics of inactivation mechanisms were direct and robust by a homozygous deletion, small deletion, or nonsense mutation. To our knowledge, our study is the first to show such frequent genetic inactivation of the *LATS2* gene in any human malignancy.

Interestingly, several MM cell lines show inactivation of both *NF2* and *LATS2*. This is in contrast to our hypothesis that the functional link between the Merlin and Hippo pathway was direct and that inactivation of each gene might be sufficient for the inactivation of the Merlin-Hippo cascade in MM cells. Indeed, although underphosphorylated, active YAP in the Y-MESO-14 cell line that had both gene inactivations was not downregulated by phosphorylation when the wild-type *NF2* gene was transduced (Fig. 4A), the cell growth of this cell line was suppressed (data not shown). In this regard, Merlin has been clearly shown to inhibit mTORC1 pathway in MM cells, with Merlin-negative MM cells displaying unregulated mTORC1 signaling and also an enhanced growth-inhibitory effect of rapamycin, an mTORC1 inhibitor (44, 45). Thus, growth suppression in Y-MESO-14 cells was likely to be induced via such signaling cascades but not via the Hippo signaling. This suggests another possibility that the main roles of Merlin for tumor-suppressive activity in MM cells reside outside the Hippo pathway regulation, that the functional link between the Merlin and Hippo pathway in MM cells is not as direct as expected, and that the simultaneous inactivation of Merlin and Hippo pathway inactivation may merely enhance MM cell growth. Furthermore, some MM cell lines with *NF2* mutation but not *LATS2* mutation also showed significant phosphorylation levels of YAP, especially at

Published OnlineFirst January 18, 2011; DOI:10.1158/0008-5472.CAN-10-2164

confluence, suggesting that the Hippo pathway in MM cells can also be activated in a Merlin-independent manner (data not shown). Thus, more detailed mechanisms of the tumor-suppressive pathways in which Merlin and LATS2 are involved must be elucidated in future studies.

The mutation frequency of *LATS2* in MM cell lines was higher than the one in primary tumors. Because most primary MM tumors contain abundant normal cells, the sensitivities of detection of allelic loss or point mutation in primary tumors are expected to be lower than those in cell lines. In this regard, among 5 primary tumors that we evaluated to have at least an allelic loss, there might be cases of homozygous deletion. Indeed, 3 of 4 tumors with an allelic loss showed the weak intensity of LATS2 staining comparable with a tumor with homozygous deletion, which suggested that both alleles of *LATS2* might be inactivated in these tumors. Thus, although the mutation frequency of 12% for *LATS2* in primary tumors was low compared with that of 35% in cell lines, we thought that one reason for this was the lower sensitivity of mutation detection. However, we could not exclude another possibility, namely, that the difference in mutation frequencies was due to selection pressure during establishment of cell lines.

In conclusion, we showed that the tumor-suppressive Hippo signaling pathway can be inactivated by *LATS2* mutation in MM cells and that LATS2 may play a critical role in regulating cell proliferation and/or survival in MM cells and nonmalignant mesothelial cells. Our result may also suggest that inhibition of activated YAP or transcription factors may serve to develop a more effective target therapy for patients with MM in the future.

Disclosure of Potential Conflicts of Interest

No potential conflicts of interest were disclosed.

Acknowledgments

We thank Dr. Adi F. Gazdar for the cell lines and Ms. Mari Kizuki and Ms. Mika Yamamoto for their excellent technical assistance.

Grant Support

This work was supported in part by a Special Coordination Fund for Promoting Science and Technology from the Ministry of Education, Culture, Sports, Science and Technology of Japan (H18-1-3-3-1), grants-in-aid for Scientific Research (B) from Japan Society for the Promotion of Science (18390245, 22300338), grant-in-aid for Third-Term Comprehensive Control Research for Cancer from the Ministry of Health, Labor and Welfare of Japan, and the Takeda Science Foundation.

The costs of publication of this article were defrayed in part by the payment of page charges. This article must therefore be hereby marked *advertisement* in accordance with 18 U.S.C. Section 1734 solely to indicate this fact.

Received June 14, 2010; revised November 30, 2010; accepted November 30, 2010; published OnlineFirst January 18, 2011

References

1. Pass HI, Vogelzang N, Hahn S, Carbone M. Malignant pleural mesothelioma. Curr Probl Cancer 2004;28:93–174.
2. Robinson BW, Lake RA. Advances in malignant mesothelioma. N Engl J Med 2005;353:1591–603.
3. Yang H, Testa JR, Carbone M. Mesothelioma epidemiology, carcinogenesis, and pathogenesis. Curr Treat Options Oncol 2008;9:147–57.
4. Ramos-Nino ME, Testa JR, Altomare DA, Pass HI, Carbone M, Bocchetta M, et al. Cellular and molecular parameters of mesothelioma. J Cell Biochem 2006;98:723–34.
5. Fennell DA, Gaudino G, O'Byrne KJ, Mutti L, van Meerbeeck J. Advances in the systemic therapy of malignant pleural mesothelioma. Nat Clin Pract Oncol 2008;5:136–47.
6. Tsao AS, Wistuba I, Roth JA, Kindler HL. Malignant pleural mesothelioma. J Clin Oncol 2009;27:2081–90.
7. Sugarbaker DJ, Richards WG, Gordon GJ, Dong L, De Rienzo A, Maulik G, et al. Transcriptome sequencing of malignant pleural mesothelioma tumors. Proc Natl Acad Sci U S A 2008;105:3521–6.
8. Ivanov SV, Miller J, Lucito R, Tang C, Ivanova AV, Pei J, et al. Genomic events associated with progression of pleural malignant mesothelioma. Int J Cancer 2009;124:589–99.
9. Gray SG, Fennell DA, Mutti L, O'Byrne KJ. In arrayed ranks: array technology in the study of mesothelioma. J Thorac Oncol 2009;4:411–25.
10. Bueno R, De Rienzo A, Dong L, Gordon GJ, Hercus CF, Richards WG, et al. Second generation sequencing of the mesothelioma tumor genome. PLoS One 2010;5:e10612.
11. Sekido Y, Pass HI, Bader S, Mew DJ, Christman MF, Gazdar AF, et al. Neurofibromatosis type 2 (NF2) gene is somatically mutated in mesothelioma but not in lung cancer. Cancer Res 1995;55:1227–31.
12. Bianchi AB, Mitsunaga SI, Cheng JQ, Klein WM, Jhanwar SC, Seizinger B, et al. High frequency of inactivating mutations in the neurofibromatosis type 2 gene (NF2) in primary malignant mesotheliomas. Proc Natl Acad Sci U S A 1995;92:10854–8.
13. Cheng JQ, Lee WC, Klein MA, Cheng GZ, Jhanwar SC, Testa JR. Frequent mutations of NF2 and allelic loss from chromosome band 22q12 in malignant mesothelioma: evidence for a two-hit mechanism of NF2 inactivation. Genes Chromosomes Cancer 1999;24:238–42.
14. Xiao GH, Gallagher R, Shetler J, Skele K, Altomare DA, Pestell RG, et al. The NF2 tumor suppressor gene product, Merlin, inhibits cell proliferation and cell cycle progression by repressing cyclin D1 expression. Mol Cell Biol 2005;25:2384–94.
15. Poulikakos PI, Xiao GH, Gallagher R, Jablonski S, Jhanwar SC, Testa JR. Re-expression of the tumor suppressor NF2/Merlin inhibits invasiveness in mesothelioma cells and negatively regulates FAK. Oncogene 2006;25:5960–8.
16. Fleury-Feith J, Lecomte C, Renier A, Matrat M, Kheuang L, Abramowski V, et al. Hemizygosity of Nf2 is associated with increased susceptibility to asbestos-induced peritoneal tumours. Oncogene 2003;22:3799–805.
17. Altomare DA, Vaslet CA, Skele KL, De Rienzo A, Devarajan K, Jhanwar SC, et al. A mouse model recapitulating molecular features of human mesothelioma. Cancer Res 2005;65: 8090–5.
18. Jongsma J, van Montfort E, Vooijs M, Zevenhoven J, Krimpenfort P, van der Valk M, et al. A conditional mouse model for malignant mesothelioma. Cancer Cell 2008;13:261–71.
19. Thurneysen C, Opitz I, Kurtz S, Weder W, Stahel RA, Felley-Bosco E. Functional inactivation of NF2/Merlin in human mesothelioma. Lung Cancer 2009;64:140–7.
20. Guled M, Lahti L, Lindholm PM, Salmenkivi K, Bagwan I, Nicholson AG, et al. CDKN2A, NF2, and JUN are dysregulated among other genes by miRNAs in malignant mesothelioma-A miRNA microarray analysis. Genes Chromosomes Cancer 2009;48:615–23.
21. Hamaratoglu F, Willecke M, Kango-Singh M, Nolo R, Hyun E, Tao C, et al. The tumour-suppressor genes NF2/Merlin and Expanded act through Hippo signalling to regulate cell proliferation and apoptosis. Nat Cell Biol 2006;8:27–36.

Published OnlineFirst January 18, 2011; DOI:10.1158/0008-5472.CAN-10-2164

22. Edgar BA. From cell structure to transcription: Hippo forges a new path. Cell 2006;124:267–73.
23. Pan D. Hippo signaling in organ size control. Genes Dev 2007;21:886–97.
24. Saucedo LJ, Edgar BA. Filling out the Hippo pathway. Nat Rev Mol Cell Biol 2007;8:613–21.
25. Zhao B, Lei QY, Guan KL. The Hippo-YAP pathway: new connections between regulation of organ size and cancer. Curr Opin Cell Biol 2008;20:638–46.
26. Overholtzer M, Zhang J, Smolen GA, Muir B, Li W, Sgroi DC, et al. Transforming properties of YAP, a candidate oncogene on the chromosome 11q22 amplicon. Proc Natl Acad Sci U S A 2006;103:12405–10.
27. Zender L, Spector MS, Xue W, Flemming P, Cordon-Cardo C, Silke J, et al. Identification and validation of oncogenes in liver cancer using an integrative oncogenomic approach. Cell 2006;125:1253–67.
28. Yokoyama T, Osada H, Murakami H, Tatematsu Y, Taniguchi T, Kondo Y, et al. YAP1 is involved in mesothelioma development and negatively regulated by Merlin through phosphorylation. Carcinogenesis 2008;29:2139–46.
29. Usami N, Fukui T, Kondo M, Taniguchi T, Yokoyama T, Mori S, et al. Establishment and characterization of four malignant pleural mesothelioma cell lines from Japanese patients. Cancer Sci 2006;97:387–94.
30. Taniguchi T, Karnan S, Fukui T, Yokoyama T, Tagawa H, Yokoi K, et al. Genomic profiling of malignant pleural mesothelioma with array-based comparative genomic hybridization shows frequent non-random chromosomal alteration regions including JUN amplification on 1p32. Cancer Sci 2007;98:438–46.
31. Goto Y, Shinjo K, Kondo Y, Shen L, Toyota M, Suzuki H, et al. Epigenetic profiles distinguish malignant pleural mesothelioma from lung adenocarcinoma. Cancer Res 2009;69:9073–82.
32. Kawaguchi K, Murakami H, Taniguchi T, Fujii M, Kawata S, Fukui T, et al. Combined inhibition of MET and EGFR suppresses proliferation of malignant mesothelioma cells. Carcinogenesis 2009;30:1097–105.
33. Tapon N, Harvey KF, Bell DW, Wahrer DC, Schiripo TA, Haber DA, et al. Salvador promotes both cell cycle exit and apoptosis in *Drosophila* and is mutated in human cancer cell lines. Cell 2002;110:467–78.
34. Scoles DR. The Merlin interacting proteins reveal multiple targets for NF2 therapy. Biochim Biophys Acta 2008;1785:32–54.
35. Baser ME. The distribution of constitutional and somatic mutations in the neurofibromatosis 2 gene. Hum Mutat 2006;27:297–306.
36. McClatchey AI, Giovannini M. Membrane organization and tumorigenesis—the NF2 tumor suppressor, Merlin. Genes Dev 2005;19:2265–77.
37. McClatchey AI, Fehon RG. Merlin and the ERM proteins—regulators of receptor distribution and signaling at the cell cortex. Trends Cell Biol 2009;19:198–206.
38. Li W, You L, Cooper J, Schiavon G, Pepe-Caprio A, Zhou L, et al. Merlin/NF2 suppresses tumorigenesis by inhibiting the E3 ubiquitin ligase CRL4(DCAF1) in the nucleus. Cell 2010;140:477–90.
39. Seidel C, Schagdarsurengin U, Blumke K, Wurl P, Pfeifer GP, Hauptmann S, et al. Frequent hypermethylation of MST1 and MST2 in soft tissue sarcoma. Mol Carcinog 2007;46:865–71.
40. Xu MZ, Yao TJ, Lee NP, Ng IO, Chan YT, Zender L, et al. Yes-associated protein is an independent prognostic marker in hepatocellular carcinoma. Cancer 2009;115:4576–85.
41. Steinhardt AA, Gayyed MF, Klein AP, Dong J, Maitra A, Pan D, et al. Expression of Yes-associated protein in common solid tumors. Hum Pathol 2008;39:1582–9.
42. Kawahara M, Hori T, Chonabayashi K, Oka T, Sudol M, Uchiyama T. Kpm/Lats2 is linked to chemosensitivity of leukemic cells through the stabilization of p73. Blood 2008;112:3856–66.
43. Strazisar M, Mlakar V, Glavac D. LATS2 tumour specific mutations and down-regulation of the gene in non-small cell carcinoma. Lung Cancer 2009;64:257–62.
44. Lopez-Lago MA, Okada T, Murillo MM, Socci N, Giancotti FG. Loss of the tumor suppressor gene NF2, encoding Merlin, constitutively activates integrin-dependent mTORC1 signaling. Mol Cell Biol 2009;29:4235–49.
45. James MF, Han S, Polizzano C, Plotkin SR, Manning BD, Stemmer-Rachamimov AO, et al. NF2/Merlin is a novel negative regulator of mTOR complex 1, and activation of mTORC1 is associated with meningioma and schwannoma growth. Mol Cell Biol 2009;29:4250–61.

The Epstein-Barr Virus Latent Membrane Protein 1 and Transforming Growth Factor–β1 Synergistically Induce Epithelial–Mesenchymal Transition in Lung Epithelial Cells

Mark D. Sides[1]*, Ross C. Klingsberg[1]*, Bin Shan[1], Kristin A. Gordon[1], Hong T. Nguyen[1], Zhen Lin[2,3,4], Takashi Takahashi[5], Erik K. Flemington[2,3,4], and Joseph A. Lasky[1]

[1]Department of Medicine, Section of Pulmonary Diseases, Critical Care and Environmental Medicine, and [2]Department of Pathology, Tulane University School of Medicine, New Orleans, LA; [3]Louisiana Cancer Research Consortium, New Orleans, LA; [4]Tulane Cancer Center, New Orleans, LA; [5]Division of Molecular Carcinogenesis, Center for Neurological Diseases and Cancer, Nagoya University Graduate School of Medicine, Showa-Ku, Nagoya, Japan

The histopathology of idiopathic pulmonary fibrosis (IPF) includes the presence of myofibroblasts within so-called fibroblastic foci, and studies suggest that lung myofibroblasts may be derived from epithelial cells through epithelial–mesenchymal transition (EMT). Transforming growth factor (TGF)–β1 is expressed and/or activated in fibrogenesis, and induces EMT in lung epithelial cells in a dose-dependent manner. A higher occurrence of Epstein-Barr virus (EBV) has been reported in the lung tissue of patients with IPF. EBV expresses latent membrane protein (LMP) 1 during the latent phase of infection, and may play a role in the pathogenesis of pulmonary fibrosis inasmuch as LMP-1 may act as a constitutively active TNF-α receptor. Our data show a remarkable increase in mesenchymal cell markers, along with a concurrent reduction in the expression of epithelial cell markers in lung epithelial cells cotreated with LMP-1, and very low doses of TGF-β1. This effect was mirrored in lung epithelial cells infected with EBV expressing LMP1 and cotreated with TGF-β1. LMP1 pro-EMT signaling was identified, and occurs primarily through the nuclear factor–κB pathway and secondarily through the extracellular signal–regulated kinase (ERK) pathway. Activation of the ERK pathway was shown to be critical for aspects of TGF-β1–induced EMT. LMP1 accentuates the TGF-β1 activation of ERK. Together, these data demonstrate that the presence of EBV-LMP1 in lung epithelial cells synergizes with TGF-β1 to induce EMT. Our *in vitro* data may help to explain the observation that patients with IPF demonstrating positive staining for LMP1 in lung epithelial cells have a more rapid demise than patients in whom LMP1 is not detected.

Keywords: latent membrane protein 1; transforming growth factor–β1; epithelial–mesenchymal transition; idiopathic pulmonary fibrosis; Epstein-Barr virus

CLINICAL RELEVANCE

A higher occurrence of detection of Epstein-Barr virus (EBV) has been noted in the lung epithelium in those with idiopathic pulmonary fibrosis (IPF) and expression of the EBV encoded latent membrane protein correlates with a poorer prognosis. This study presents possible molecular mechanism for the contribution of EBV to the progression of IPF.

Idiopathic pulmonary fibrosis (IPF) is characterized by the presence of myofibroblasts that deposit collagen, resulting in destruction of the alveolar architecture and progressive loss of lung function (1). IPF is a condition of unknown etiology, with the possibility of multiple factors implicated in the pathogenesis. Recurring alveolar epithelial injury with subsequent recruitment and/or activation of fibroblasts/myofibroblasts has been suggested as a pathogenic mechanism of IPF (2, 3).

An association between the Epstein-Barr virus (EBV) and IPF has been proposed (4), and EBV has been detected in the lungs of patients with IPF at a higher rate than in control populations in subsequent studies (5–9), which raises the question of how EBV may be involved in the pathogenesis of IPF. EBV expresses few proteins during the latent phase of infection, including the group of nuclear antigens, Epstein-Barr Nuclear Antigens (EBNA), and two membrane proteins—latent membrane protein (LMP) I and II. The expression of the EBV LMP1 in the lung epithelium of patients with IPF correlated with a poorer prognosis (8). LMP1 is a six-pass transmembrane protein that mimics a constitutively active member of the TNF receptor superfamily, and activates, among others, the nuclear factor (NF)–κB (10) and extracellular signal–regulated kinase (ERK) (11) pathways. Exogenous expression of LMP1 has been shown to induce phenotypic changes (12), stress fiber formation (13), and epithelial–mesenchymal transition (EMT) (14) in nasopharyngeal epithelial cells.

EMT can be defined as a series of events during which epithelial cells lose many of their epithelial characteristics and take on properties that are typical of mesenchymal cells. Hallmarks of EMT include the loss of epithelial markers, such as adherent junctions and expression of E-cadherin (E-Cad), and tight junctions and expression of zona occludens (ZO)–1. Concomitantly, EMT involves a gain of mesenchymal proteins, such as vimentin and N-cadherin (N-Cad), along with cytoskeletal remodeling with a gain of filamentous actin stress fibers, increase in expression of extracellular matrix proteins, such as fibronectin (Fn) and collagen 1, and the expression of matrix metalloproteinases (MMPs) and plasminogen activation inhibitor (PAI)–1. EMT has been implicated in the pathology of cancers and fibrosis, although the exact mechanism or extent is variable (for

(Received in original form June 29, 2009 and in final form July 15, 2010)

* These authors contributed equally to this work.

This work was supported by National Institutes of Health grant RO1HL083901 (J.A.L.) and Louisiana Board of Regents Louisiana Educational Quality Support Fund (2008–10)-RD-A-26 (B.S.), and by Louisiana Board of Regents RSGS grant LEQSF (2006–11)GF06 (M.S.).

Correspondence and requests for reprints should be addressed to Joseph A. Lasky, M.D., Tulane University School of Medicine, Department of Pulmonary Medicine and Critical Care–SL9, 1430 Tulane Avenue, New Orleans, LA 70112. E-mail: jlasky@tulane.edu

This article has an online supplement, which is accessible from this issue's table of contents at www.atsjournals.org

Am J Respir Cell Mol Biol Vol 44. pp 852–862, 2011
Originally Published in Press as DOI: 10.1165/rcmb.2009-0232OC on August 6, 2010
Internet address: www.atsjournals.org

review, *see* Ref. 15). The process of EMT provides support for the model of disregulated epithelial repair in IPF. In a murine model of lung fibrosis, where β-galactosidase was expressed exclusively on the surfactant protein (SP)–C promoter, myofibroblasts were found to be β-galactosidase positive, suggesting a role of EMT in lung fibrogenesis (16). In addition, there is immunohistochemical evidence for EMT in IPF lung (17).

Transforming growth factor (TGF)–β1 is an essential cytokine in development and normal immune modulation (18). The canonical TGF-β1 cascade initiates with ligand binding and homodimerization of the type I and type II transmembrane receptors. The receptor Smads (rSmad), Smad2 and/or Smad3, complex with Smad anchor for receptor activation (SARA) and cytoplasmic promyelocytic leukemia protein (cPML) in association with the TGF-β1 receptor to allow for phosphorylation and activation of rSmad (19). Once phosphorylated, rSmad dimerizes with the co-Smad (Smad4), and translocates to the nucleus, where the complex regulates the transcription of Smad-responsive genes. Expression of the inhibitory Smad, Smad7, is increased by Smad 2/3 activation, and functions as a negative feedback loop to regulate TGF-β1 signaling (20). TGF-β1 has been implicated in fibrosis of a variety of tissues, including lung (21), and has been shown to induce EMT in lung epithelial cells in a time- and dose-dependent manner (22). In addition, the presence of EBV in lung epithelial cells has been reported to increase transcription of TGF-β1 (23). Overexpression of TGF-β1 by adenoviral vector in mice results in pulmonary fibrogenesis (16).

In this study, the effects of LMP1 on TGF-β1–induced EMT were investigated using lung epithelial cells. At concentrations of TGF-β1 below the threshold to cause EMT, LMP1 sensitizes the cells to a TGF-β1–induced EMT response, inducing dramatic phenotypic changes with concurrent loss of epithelial markers and increased cellular motility. This synergistic effect was also observed in lung epithelial cells infected with EBV and cotreated with TGF-β1. LMP1 reduces TGF-β1 signaling through Smads in favor of the ERK pathway. Inhibition of ERK activation abrogated the TGF-β1 contribution to EMT, and partially inhibited LMP1-induced EMT. The contribution of LMP1 to this synergistic effect was blocked by inhibiting the NF-κB pathway. The dramatic sensitization to TGF-β1–induced EMT by LMP1 may help to explain the observation that patients with IPF demonstrating positive staining for LMP1 in alveolar epithelial cells have a more rapid demise than that observed in patients in whom LMP1 is not detected.

MATERIALS AND METHODS

Cell Culture

A549 and HPL1D cells were cultured as previously described (24, 25). During treatment with recombinant human TGF-β1 (R&D Systems, Minneapolis, MN), A549 cells were cultured in Dulbecco's modified Eagle's medium plus 0.5% FBS. Generation of the pEhyg*FLAG*LMP1*wt vector and retroviral transduction of cells have been described previously (26). During treatments longer than 72 hours, media were changed every 48 hours.

Plasmids and Reagents

The pcDNA*Flag*LMP1*wt vector was provided by Nancy Rabb-Traub (University of North Carolina, Chapel Hill, NC). Dominant active-IκB (DAIκB) plasmid (27) was provided by Dean Ballard (Vanderbuilt University School of Medicine, Nashville, TN). U0126 was purchased from Promega (Madison, WI). The green fluorescent protein (GFP) adenovirus was a gift from J. K. Kolls (Louisiana State University, New Orleans, LA). The LMP1 adenovirus (28) was provided by S. Gottschalk (Baylor University School of Medicine, Houston, TX). RT^2-PCR primers were purchased from Integrated DNA Technologies (36B4, E-Cad, PAI-1, MMP9, vimentin, collagen 1 [25], Fn, alpha smooth muscle actin (aSMA) [29], Snail, Slug, and ZEB-1 [30]; Coralville, Iowa) or SA Bioscience (Smad 7, SP-C; Frederick, MD).

Establishment of EBV-Infected A549 Cells

A549 cells were infected with recombinant EBV using the cell–cell infection method. Akata-BX.1 cells (31) (provided by Lindsay Hutt-Fletcher, Louisiana State University, Shreveport, LA) were activated with goat anti-human IgG (Sigma, St. Louis, MO) for 24 hours. Activated Akata-BX.1 cells were applied directly to the A549 cells for 48 hours. At 24 hours after infection, media were replaced with fresh media containing 500 μg/ml G418 (Invitrogen, Carlsbad, CA).

Adenovirus Infection

Cells were inoculated at a multiplicity of infection of 20. A549 cells were treated with TGF-β1 24 hours after infection. HPL1D cells were treated with TGF-β1 48 hours after infection.

Antibodies

Antibodies to E-Cad, Smad2, β-actin, ERK, phosphorylated ERK, phosphorylated Smad2 Smad3, and phosphorylated Smad3 were purchased from Cell Signaling (Western blot, 1:1,000; inflorescence, 1:200; Danvers, MA). Antibodies to LMP1, Smad2/3, and vimentin were purchased from BD Bioscience (1:1,000; San Diego, CA). Antibodies to Twist, PML, SARA, and N-Cad were purchased from Santa Cruz (1:200; Santa Cruz, CA). Antibody to aSMA was purchased from Sigma (1:10,000). Antibody to fibronectin extra domain A (Fn-EDA) was purchased from AbCam (1:200; Cambridge, MA). Antibody to ZO-1 was purchased from ZyMed/Invitrogen (1:500). Secondary antibodies used were IRDye 680 goat anti-mouse IgG or IRDye 800CW goat anti-rabbit IgG (LiCor, Lincoln, NE). Secondary antibodies used for immunofluorescence were Alexa Fluor 594 goat anti-rabbit and Alexa Fluor 488 goat anti-rabbit (1:500; Invitrogen). Stress fibers were stained using Alexa Fluor 488 conjugated to phalloidin (Invitrogen).

Gelatin Zymography

Gealtin zymography was performed as previously described (32), with the exception that 30 μl of unconcentrated conditioned medium was used per sample.

Migration Assay

Retrovirally transduced A549 cells were stained with Calcein AM (Molecular Probes/Invitrogen) and plated in HTS FluoroBlok insert (BD Falcon, Franklin Lakes, NJ) in Dulbecco's modified Eagle's medium with or without TGF-β1. Full medium was used as chemoattractant. Invading cells were measured by fluorescence at 6 hours.

Statistical Analysis

Comparisons were analyzed by ANOVA using the modified Bonferroni *post hoc* test. Data presented are representative of multiple experiments performed in triplicate, and are presented as the mean (±SEM).

RESULTS

Coexposure to Low-Dose TGF-β1 and LMP1 Induced Morphological Changes in A549 Cells

A549 cells display an epithelial morphology in culture. Exposure to either LMP1 or 1 ng/ml TGF-β1 for 48 hours results in morphological changes in a low percentage of the cells where coexposure results in a complete loss of the typical "cobblestone" morphology and the appearance of a spindle shape (Figure 1, Phase). To investigate the loss of adherent and tight junctions typical of the epithelial phenotype, cells were stained for E-Cad and ZO-1 using immunofluorescence. TGF-β1 and LMP1 independently reduced the intensity of E-Cad, although the distinct cell outlines of adherent junctions were still evident, whereas coexposure resulted in a complete loss of E-Cad signal (Figure 2, E-Cad). Similarly, LMP1 reduced the intensity of the

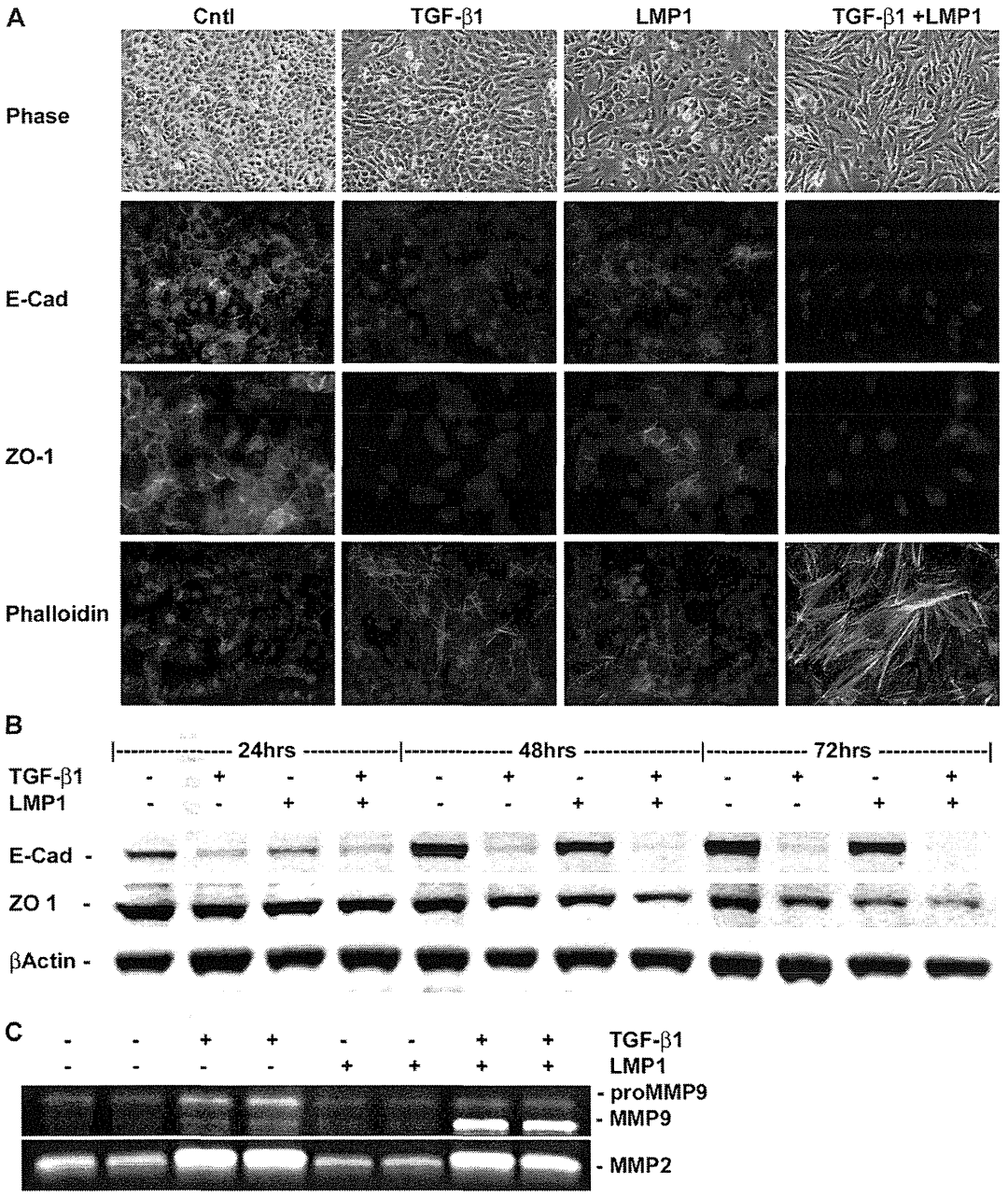

Figure 1. Latent membrane protein (LMP) 1 enhanced the transforming growth factor (TGF)–β1–induced phenotypic change and loss of epithelial markers in A549 cells. (*A*) Phase–contrast and immunofluorescence staining of A549 cells treated with 1 ng/ml TGF-β1 for 48 hours with and without LMP1. Adherent junctions are imaged by E-cadherin (E-Cad) staining; tight junctions are imaged by zona occludens (ZO)–1 staining, and filamentous actin of stress fibers are imaged by phalloidin staining. (*B*) Western blot analysis of A549 cell lysates collected at the indicated time points after transfection and cotreatment with 1 ng/ml TGF-β1. (*C*) Gelatin zymography of A549 conditioned media obtained 48 hours after treatment with 1 ng/ml TGF-β1 with and without LMP1. MMP, matrix metalloproteinase. $*P < 0.05$ compared with control; $**P < 0.01$ compared with control; $***P < 0.001$ compared with control.

ZO-1 signal, whereas the tight junction structures were maintained. TGF-β1 alone or in conjunction with LMP1 resulted in a loss of ZO-1 signal and tight junction structure (Figure 1, ZO-1). Concurrent with the loss of cell–cell structure, TGF-β1 or LMP1 independently promoted the minimal formation of stress fibers, and coexposure resulted in the formation of abundant stress fibers (Figure 1. Phalloidin). The loss of E-Cad and ZO-1 with coexposure was verified by Western blot (Figure 1B). In addition, an increase in the levels of secreted MMP2 and MMP9 were detected in the conditioned medium of both LMP1 and TGF-β1–treated cells. The level of activated MMP9 was dramatically up-regulated in the conditioned medium of coexposed cells (Figure 1C).

Coexposure to Low-Dose TGF-β1 and LMP1 Induced Transcriptome Changes in A549 Cells

To determine if the loss of E-Cad and gain of MMP9 proteins were due to transcriptional regulation, mRNA was harvested at 24 hours after treatment and analyzed by real-time qRT-PCR. TGF-β1 treatment resulted in a loss of E-Cad transcription, whereas expression of LMP1 did not. Coexposure resulted in a twofold loss in E-Cad mRNA level when compared with TGF-β1 exposure alone (Figure 2A). Similarly, whereas exposure to TGF-β1 or LMP1 increased MMP9 mRNA levels by 80-fold and 40-fold, respectively, coexposure resulted in an increase of 3,400-fold (Figure 2C). The expression of PAI-1 increased with exposure to TGF-β1 or LMP1 independently, and showed an additive increased with coexposure (Figure 2B).

LMP1-Enhanced Cellular Mobility in Response to TGF-β1–Induced EMT

The ability of LMP1 and TGF-β1 cotreatment to affect cell migration was assessed using the FluoroBlok migration assay (Figure 2D). Treatment with TGF-β1 alone increased migration by roughly twofold, whereas LMP1 expression increased migration approximately threefold. Cotreatment induced a synergistic effect, increasing cell migration by approximately ninefold.

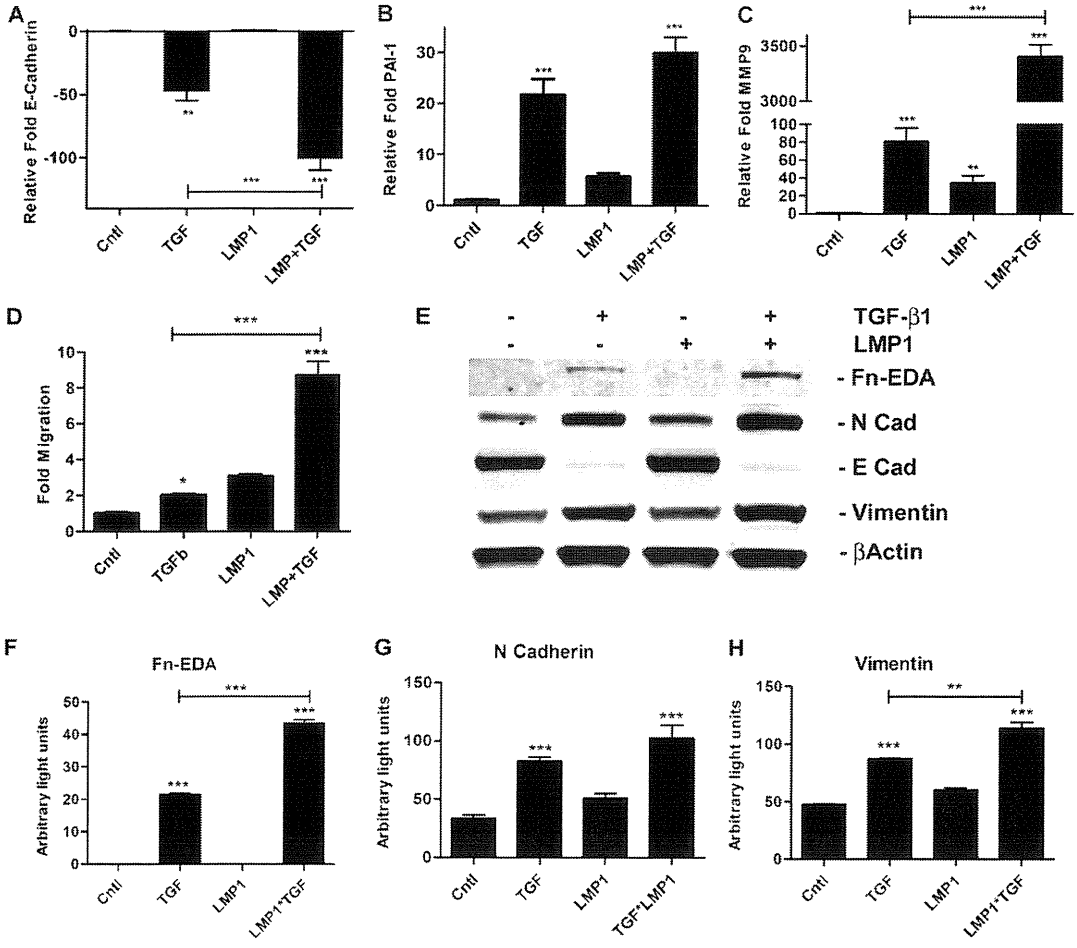

Figure 2. LMP1 enhanced the TGF-β1–induced gain of mesenchymal markers. Real-time quantitative RT-PCR (real-time qRT-PCR) analysis of expression of (*A*) E-Cad, (*B*) plasminogen activation inhibitor (PAI)–1, and (*C*) MMP9 at 24 hours after treatment with 1 ng/ml TGF-β1 with and without LMP1 expression. (*D*) Migration assay of TGF-β1–treated A549 cells with and without LMP1 expression. (*E*) Western blot of A549 cell lysates collected 4 days after transfection and cotreatment with 1 ng/ml TGF-β1. (*F–H*) Densitometric analysis of three separate Western blots, of which Figure 1E is representative. Cntl, control; Fn-EDA, fibronectin–Extra Domain A. $^{*}P < 0.05$ compared with control; $^{**}P < 0.01$ compared with control; $^{***}P < 0.001$ compared with control.

Coexposure to Low-Dose TGF-β1 and LMP1 Induced a Gain of Mesenchymal Markers in A549 Cells

To determine if the loss of epithelial markers in A549 cells exposed to TGF-β1 and LMP1 was accompanied by a gain in mesenchymal markers, cells were exposed for 4 days and analyzed by Western blot (Figure 2E). Exposure to TGF-β1 resulted in a gain in the mesenchymal markers, N-Cad (Figure 2G) and vimentin (Figure 2H), as well as the fibrotic marker, Fn-EDA. Coexposure with LMP1 resulted in an additive increase in both N-Cad and vimentin, whereas the presence of LMP1 increased induction of Fn-EDA by TGF-β1 more than twofold (Figure 2F).

Immortalized Primary Cell Response to LMP1 and TGF-β1 Mirrored that of A549 Cells

To determine whether the phenotypic changes seen in A549 cells were cancer cell–specific, the experiments were repeated using the immortalized primary cell line, HPL1D. Consistent with the results seen in A549 cells, levels of ZO-1 and E-Cad were reduced in HPL1D cells exposed to LMP1 or TGF-β1 independently, with a complete loss in coexposed cells (Figure 3A) at 48 hours after treatment. Levels of Fn-EDA were increased with TGF-β1 treatment, which was enhanced by coexposure. At the transcription level, treatment with TGF-β1 resulted in suppression of E-Cad that was synergistically enhanced by LMP1 expression (Figure 3B), whereas the increase in transcription of PAI-1 was found to be TGF-β1 dependent in HPL1D cells.

To determine the extent to which HPL1D cells might complete the transition to a mesenchymal phenotype, cells were coexposed for 7 days. Cotreatment with TGF-β1 and LMP1 resulted in an increase the mesenchymal markers, aSMA and N-Cad proteins (Figure 3D). Gelatin zymography analysis displayed a substantial increase in MMP9 expression with cotreatment (Figure 3E). In addition, cotreatment with TGF-β1 and LMP1 resulted in the synergistic up-regulation of MMP9 mRNA similar to that seen in A549 cells (Figure 3I).

At the transcription level, 7-day exposure to TGF-β1 or LMP1 alone resulted in a loss of expression of the epithelial types II marker, SP-C, whereas coexposure resulted in an additive loss (Figure 3F). Expression of the mesenchymal marker, Fn (Figure 3G), as well as the fibrotic markers, Fn-EDA (Figure 3H) and collagen 1 (Figure 3K), were increased by TGF-β1 treatment and enhanced with cotreatment with LMP1.

Effects of LMP1 Expressed from the EBV Genome Mirrored Those of LMP1 Transient Transfection and Retroviral Transduction in a Dose-Dependent Manner

To investigate the effects of LMP1 expressed at biological levels and in the context of coexpression with the EBV latent proteome, A549 cells were infected with the recombinant EBV strain, BX. Expression levels of LMP1 were determined by Western blot (Figure 3L), and cells from two separate infections differentially expressing LMP1 were exposed to 1 ng/ml TGF-β1 for 48 hours. EBV-infected cells expressing LMP1 at low levels (2C) responded similarly to uninfected parental A549 cells (U) with equally lower E-Cad expression and increased expression of vimentin. TGF-β1 treatment of cells expressing a greater amount of LMP1 (3A) resulted in a greater loss of E-Cad and gain in vimentin when compared with either the 2C cell line or uninfected parental cells (Figure 3M).

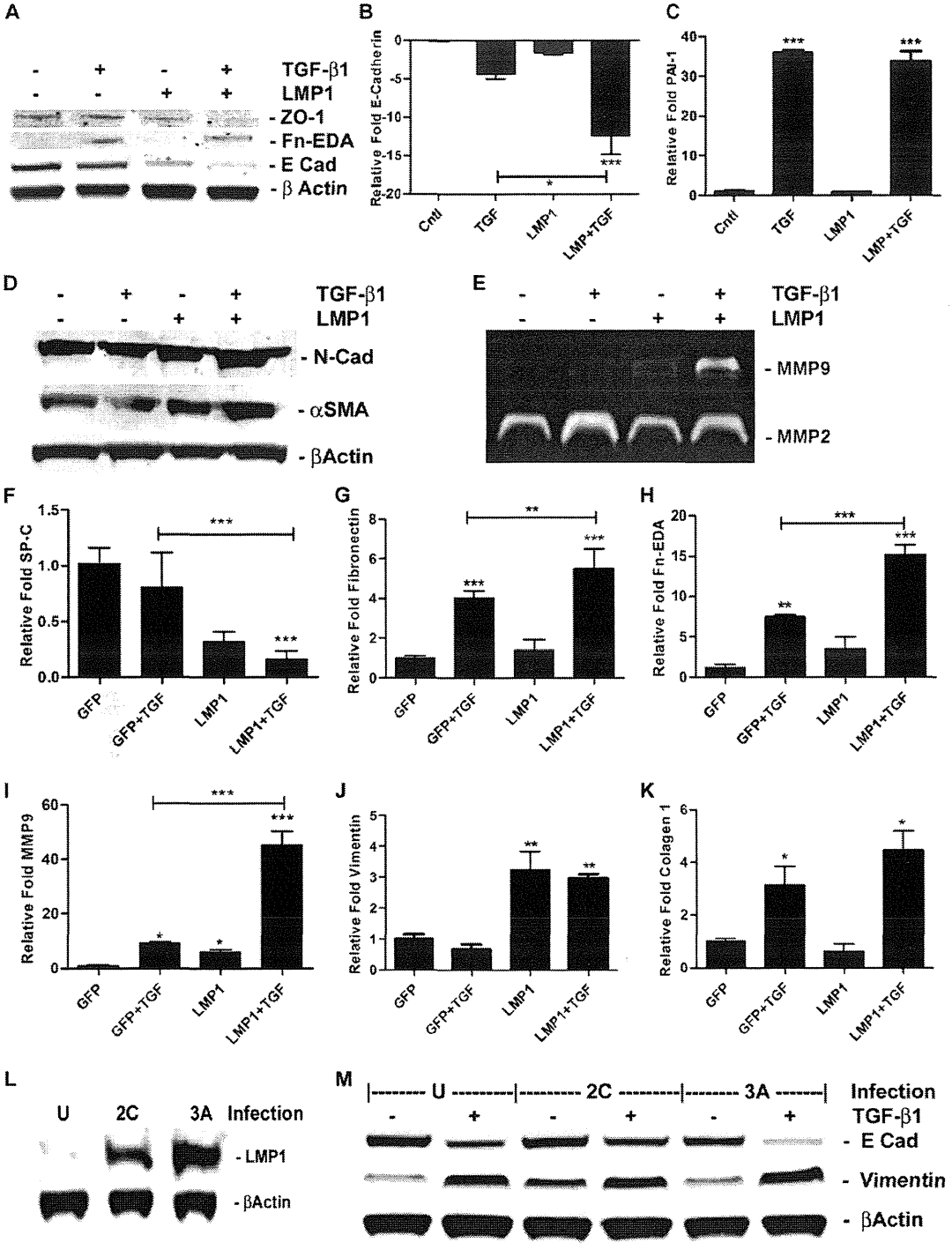

Figure 3. The response to LMP1 and TGF-β1 treatment in primary cell line mirrored that of A549 cells. (*A*) Western blot analysis of HPL1D cell lysates collected 96 hours after infection with adenovirus (multiplicity of infection 20) expressing either green fluorescent protein or LMP1 and 48 hours of cotreatment with 1 ng/ml TGF-β. Real-time real-time qRT-PCR of (*B*) E-Cad and (*C*) PAI-1 mRNA levels 72 hours after infection with adenovirus expressing GFP or LMP1 and 24 hours after cotreatment with 1ng/ml TGF-β1. (*D*) Western blot of HPL1D cells 7 days after treatment with 1 ng/ml TGF-β1 and 9 days after infection with either the GFP or LMP1 expression adenovirus. (*F–K*) RT2-PCR of the indicated mRNA expression in HPL1D cells 7 days after treatment with 1 ng/ml TGF-β1 and 9 days after infection with either the GFP or LMP1 expression adenovirus. Effects of LMP1 expressed from the Epstein-Barr virus (EBV) genome mirror those of LMP1 transient transfection and retroviral transduction in a dose-dependent manner. (*L*) Western blot analysis of cell lysates from uninfected parental A549 cells (U) or A549 cells infected with the recombinant EBV strain, BX1 (clones 2C, 3A), 48 hours after treatment with 1 ng/ml TGF-β1 (where indicated). (*M*) Western Blot of LMP1 expression in the two EBV-BX1–infected A549 cell lines. $^{*}P < 0.05$ compared with control; $^{**}P < 0.01$ compared with control; $^{***}P < 0.001$ compared with control.

LMP1 Inhibited TGF-β1 Activation of the Smad Pathway

The canonical TGF-β1 signaling cascade involves phosphorylation of Smad2 and/or Smad3 by the TGF-β1 receptor (18). To investigate the role of Smad phosphorylation in the phenotypic change seen with TGF-β1 and LMP1 cotreatment, cells were transiently transfected with either the LMP1 expression or empty vector, exposed to 1 ng/ml TGF-β1, and the levels of phosphorylated Smad assessed by Western blot (Figure 4A). Exposure to TGF-β1 resulted in a robust increase in Smad 2 phosphorylation as early as 10 minutes that peaked at 60 minutes and diminished thereafter, whereas Smad 3 phosphorylation peaked at 30 minutes and was less robust. With coexposure, however, Smad 2 phosphorylation peaked at 30 minutes at a greatly reduced level compared with TGF-β1 exposure alone. Smad3 phosphorylation was reduced with coexposure and peaked at 60 minutes. To determine whether the reduction in Smad phosphorylation reduced expression of a Smad-responsive gene, the Smad-responsive, but LMP1-unresponsive, SMAD7 gene was analyzed by real-time qRT-PCR. Expression of LMP1 alone did not affect expression of Smad7, whereas exposure to TGF-β1 increased expression of Smad7 by twofold at 24 hours in A549 cells (Figure 4B), and 12-fold at 4 days in HPL1D cells (Figure 4C). Expression of LMP1 greatly reduced the TGF-β1–induced increase in Smad7 in both A549 and HPL1D cells.

The cytoplasmic isoform of the cPML has been shown to be essential for TGF-β1 signaling (19). The levels of cPML were analyzed in A549 cells retrovirally transduced with either the empty vector or two separate transductions differentially

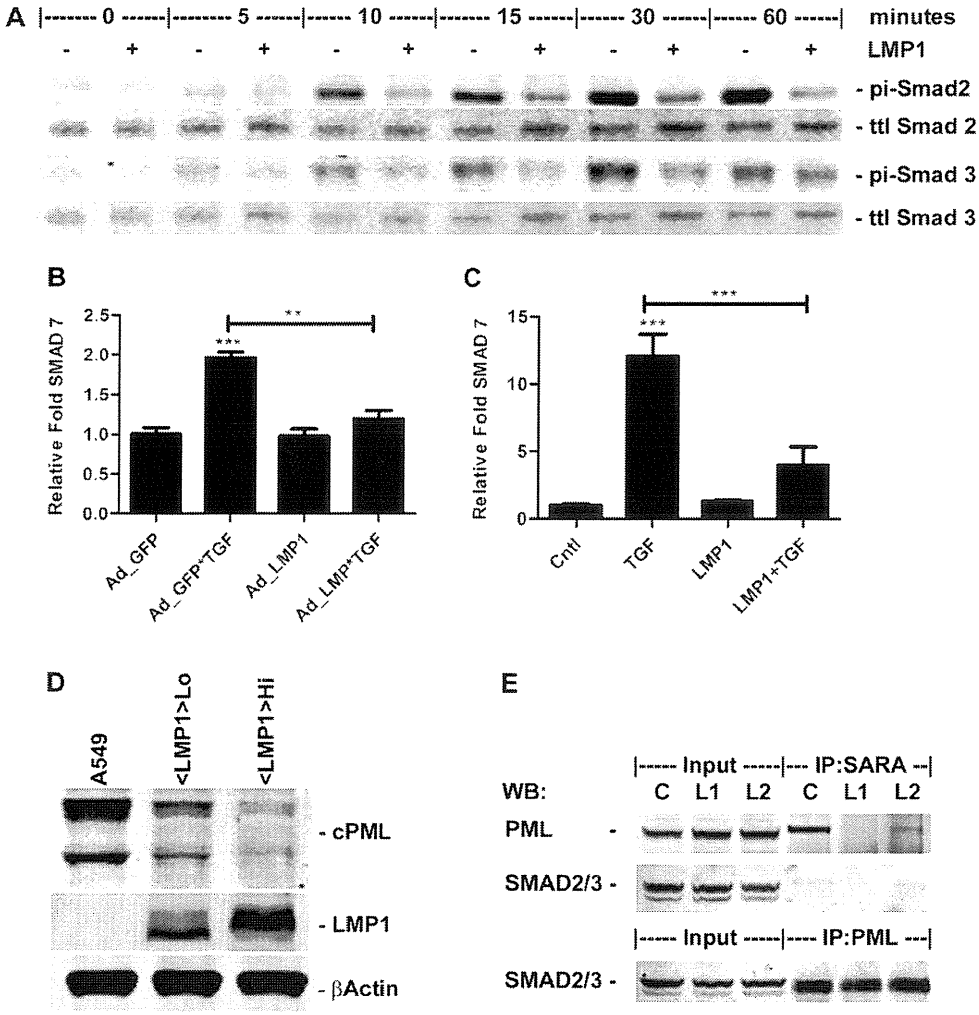

Figure 4. LMP1 inhibits TGF-β1 signaling through the Smad pathway. (*A*) Western blot of cell lysates collected at specified time points after treatment with 1 ng/ml TGF-β1 with and without LMP1 expression. RT2-PCR of Smad7 mRNA expression levels in (*B*) A549 cells 24 hours after treatment with 1 ng/ml TGF-β1 and 72 hours after infection with either GFP or LMP1 expression adenovirus (MOI20), or (*C*) HPL1D cells 48 hours after treatment with 1 ng/ml TGF-β1 and 96 hours after infection with either GFP or LMP1 expression adenovirus (MOI20). (*D*) Western blots of cell compartmental fractions from A549 cells retrovirally transduced with either the empty vector or two separate transductions with the LMP1 expression vector expressing different levels of LMP1. (*E*) Western blot analysis of Smad anchor for receptor activation (SARA) immunoprecipitation reactions from retrovirally transduced cells detailed in (*D*). Ad, adenovirus; cPML, cytoplasmic promyelocytic leukemia protein; pi, phosphorylated; ttl, total; WB, Western blot. $^{**}P < 0.01$ compared with control; $^{***}P < 0.001$ compared with control.

expressing LMP1 (Figure 4D). LMP1 was found to reduce the level of cPML in a dose-responsive manner. To investigate whether the reduction in cPML affected the cPML–SMAD–SARA signaling complex, immunoprecipitation experiments were conducted (Figure 4E). Immunoprecipitation of SARA displayed a reduction in interaction between SARA and cPML in the presence LMP1.

LMP1 Expression Reduced Expression of Twist, but Did Not Affect Expression of Snai1, Slug, or ZEB1

To investigate whether LMP1 alters expression of the classical E-Box–binding inducers of EMT, Snai1, Slug, and ZEB1 expression were analyzed by real-time qRT-PCR (Figure 5A). Treatment with TGF-β1 resulted in increased expression of all three gene products, although expression was unaffected by LMP1 alone or when LMP1 was combined with TGF-β1. LMP1 has been reported to induce EMT in MDCK cells through the increased expression of Twist (14). Cells were transiently transfected with either the LMP1 expression or empty vector and cotreated with TGF-β1 for 1, 2, and 3 days, and Twist expression analyzed by Western blot analysis to investigate whether LMP1 affected the expression of Twist in A549 cells (Figure 5B). Although TGF-β1 exposure did not affect the expression of Twist at any time point, LMP1 reduced Twist protein in a time-dependent manner. Stable expression of LMP1 by retroviral transduction resulted in a complete loss of Twist protein.

LMP1-Enhanced TGF-β1 Activation of ERK Pathway

Activation of the ERK pathway has been reported to be essential for LMP1-induced EMT (11). To investigate the possible cooperative activation of the ERK pathway by LMP1 and TGF-β1, cells were transiently transfected with either the LMP1 expression or empty vector, and cotreated with TGF-β1. ERK phosphorylation was determined by Western blot (Figures 6A and 6B). LMP1 expression increased ERK phosphorylation through the time course of the study. TGF-β1 exposure increased ERK phosphorylation as early as 15 minutes, peaked at 30 minutes, and remained above baseline through 48 hours. With cotreatment, ERK activation increased at 15 minutes when compared with LMP1 expression alone, and was significantly increased at 15 and 30 minutes. Through 72 hours, cotreatment increased phosphorylation of p42, although the increase was subtle as determined by densitometric analysis (Figure E2).

Inhibition of ERK Phosphorylation Protected from LMP1- and TGF-β1–Induced EMT

To investigate whether activation of the ERK pathway was essential to TGF-β1– and/or LMP1-induced EMT, the small molecule inhibitor of ERK phosphorylation, U0126, was used. A dose of 50 μM U0126 was required to inhibit phosphorylation of ERK by either TGF-β1 or LMP1 alone, although this concentration did not completely abrogate ERK phosphorylation in response to coexposure (Figure 6C). The reduction in

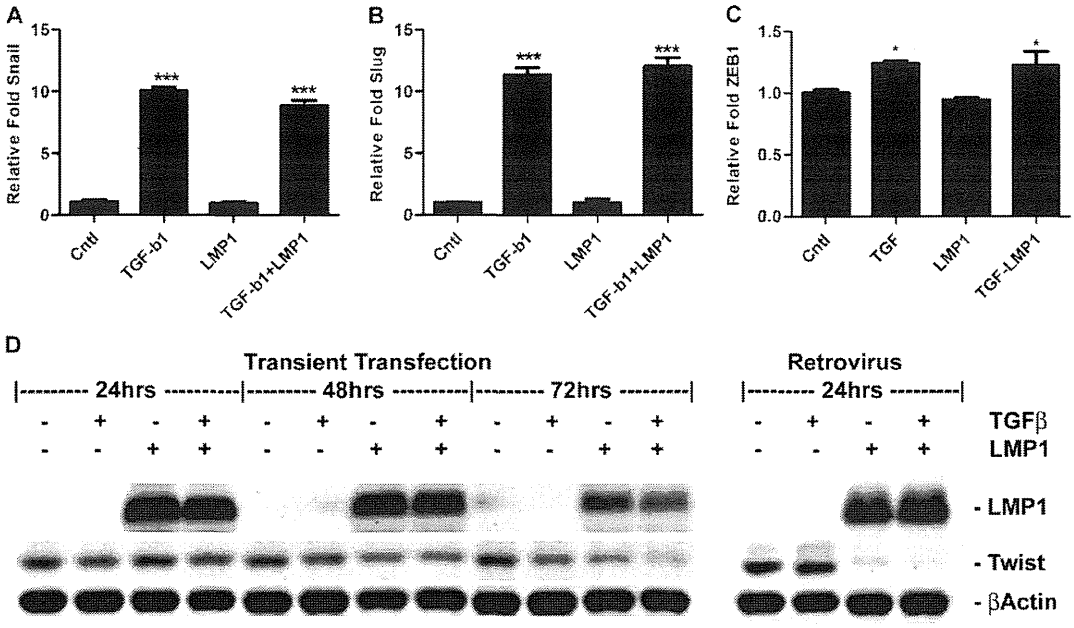

Figure 5. LMP1 does not affect expression of E-Box–binding transcription repressors. (*A*–*C*) Real-time qRT-PCR of mRNA levels of transcription repressors Snai1, Slug, and ZEB1 from mRNA isolated at 24 hours after transfection and cotreatment with 1 ng/ml TGF-β1. (*D*) Western blot analysis of Twist expression in cell lysate from time points indicated after transfection and cotreatment with 1 ng/ml TGF-β1. $*P < 0.05$ compared with control; $***P < 0.001$ compared with control.

ERK phosphorylation resulted in concomitant protection from loss of E-Cad expression. U0126 treatment blocked the TGF-β1 or LMP1 loss of expression, but was insufficient to protect from the loss expression by cotreatment. Inhibition of ERK phosphorylation, however, was sufficient to protect against the TGF-β1–induced increase in expression of MMP2 and MMP9, whereas the up-regulation of MMP9 with coexposure was greatly diminished (Figures 6D and 6G). Inhibition of ERK phosphorylation prevented the loss of E-Cad expression associated with TGF-β1 exposure and TGF-β1/LMP1 coexposure (Figure 6E), although expression of Snai1 and Slug was not completely reduced to baseline (Figures 6H and 6I). Expression of PAI-1 was unaffected by inhibition of ERK phosphorylation (Figure 6F).

Inhibition of NF-κB Activation Protected against LMP1-Induced EMT

To assess the relative contribution of NF-κB pathway activation in TGF-β1– and LMP1-induced EMT, LMP1 was coexpressed with a dominant active IκB construct (ΔAIκB). Inhibition of NF-κB activation had no effect on E-Cad expression with TGF-β1 or LMP1 individually or with coexposure. The LMP1 effect of up-regulating MMP9 and PAI-1, alone or with TGF-β1-coexposure, was mitigated to either baseline or to that of TGF-β1 exposure alone (Figures 7A–7C). The inhibition of NF-κB activation was verified by an NF-κB–responsive luciferase assay (Figure 7E). Expression of the ΔAIκB abrogated luciferase activity at baseline as well as with TNF-α stimulation.

DISCUSSION

The clinical decline in patients afflicted with IPF is variable, and may conceivably be modified by the lung microbiome. The model of epithelial injury and disregulated repair provides a central mechanism on how viral infection may modulate lung fibrogenesis (3, 33). The reported presence of Herpeviridae in the type II alveolar epithelial cells of patients with IPF suggests a role for herpes viral infection in the progression of IPF. The concept of epithelial cell damage by viral lytic-phase replication has already been explored (2), but little is known about the effects of stable latent viral infection on the behavior of lung epithelial cells. Our data provide a molecular mechanism through which the presence of LMP1 in the lung epithelium predisposes cells to undergo EMT by enhancing signaling through the ERK pathway.

Treatment of cells expressing LMP1 with low-dose TGF-β1 resulted in morphological changes, a loss of epithelial markers, a gain of mesenchymal markers, enhanced motility, and increased expression of fibrotic markers. Cotreatment with TGF-β1 and LMP1 resulted in a disruption of adherent and tight junctions, with loss of expression of E-Cad and ZO-1, as well as the loss of the type II pneumocyte marker, SP-C. Subsequently, a gain was observed in the mesenchymal markers, N-Cad, vimentin, and Fn, as well as an increase in expression of PAI-1 and MMP9, and the formation of stress fibers. These data demonstrate a completion of the transition from epithelial phenotype to mesenchymal phenotype. In addition, the induction of fibrotic markers, such as aSMA, Fn-EDA, and collagen 1, support a fibrogenic phenotype.

The predominant model of EBV-infected lung epithelium used in this study involved A549 cells transiently transfected with an LMP1 expression plasmid. LMP1 was expressed in the primary cell line, HPL1D, to validate this model. Expression of LMP1 with and without treatment with TGF-β1 in HPL1D cells mirrored that of LMP1 expression in A549 cells, although the response was less robust. This is consistent with the published report of comparative TGF-β1 responsiveness in the HPL1D cell line (34). To validate both the expression levels and function of LMP1 in the context of the EBV virus, A549 cells were infected with the BX-1 strain of EBV and exposed to TGF-β1. The EBV-infected cells mimicked the LMP1-positive A549 cells in the response to TGF-β1 treatment, with loss of E-Cad and increase in vimentin expression in an LMP1 dose–dependent manner. These data support the expression of LMP1 in A549 cells as an appropriate model of LMP1-positive EBV latency in lung epithelial cells in the context of TGF-β1–induced EMT. Although LMP1 and TGF-β1 treatment independently induce EMT at higher doses (TGF-β1) or later time points (TGF-β1, LMP1), our goal was to investigate the possible cooperative effect of LMP1 and TGF-β1 in fostering EMT. The capacity of TGF-β1 to induce EMT (22), and the presence of EMT in IPF (21), has been reported. In this study, 1 ng/ml TGF-β1 treatment was insufficient to fully induce EMT in A549 cell within 72 hours, as judged by morphological changes

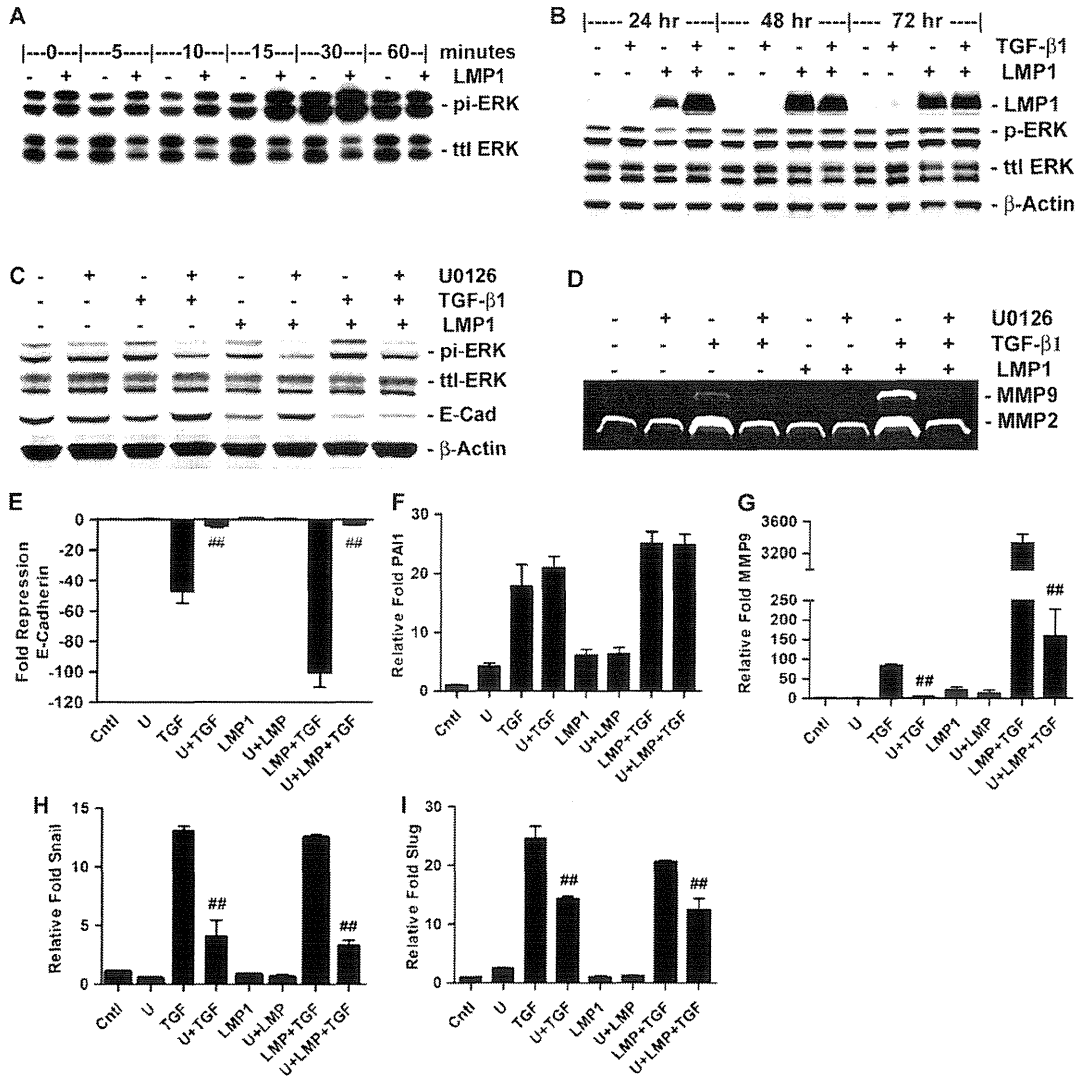

Figure 6. LMP1 enhances TGF-β1–induced extracellular signal–regulated kinase (ERK) activation. (*A* and *B*) Western Blot analysis of phosphorylated ERK1/2 using cell lysate obtained over a timecourse after transfection and cotreatment with TGF-β1. (*C*) Western blot analysis of A549 cell lysates. A549 cells were treated with 50 μm U0126 for 3 hours before treatment with 1 ng/ml TGF-β1 for 48 hours. (*D*) Gelatin zymography analysis of MMP levels in conditioned media from cells in (*C*). (*E–I*) Real-time qRT-PCR of MMP9, E-Cad, PAI-1, and E-Box–binding protein mRNA levels 24 hours after transfection and cotreatment with TGF-β1 and U0126. $^{\#\#}P < 0.01$ inhibitor compared with condition without inhibitor.

and loss of the epithelial cell marker, E-Cad. LMP1 has been reported to induce the formation of stress fibers (13) and EMT in epithelial cells (12, 14). In transient transfection experiments, expression of LMP1 was titrated so as not to fully induce EMT, although, at later time points, where cells were retrovirally transduced and expressed very large amounts of LMP1, LMP1 did independently induce EMT, consistent with published reports.

In our model of latent EBV infection, LMP1 primes the cell for a TGF-β1 response. The dramatic change in cell morphology and protein expression in LMP1-positive cells treated with low-dose TGF-β1 demonstrated a high level of synergy between LMP1 and TGF-β1. Phosphorylation and activation of the ERK pathway has been shown to be essential in TGF-β1–induced EMT in normal murine mammary gland epithelial cells and mouse cortical tubule epithelial cells (35), whereas LMP1 activation of the ERK pathway through the C-terminus activation region-1 domain has been implicated in the regulation of cellular motility and invasion in a variety of epithelial cells (11). In our system, LMP1 constitutively activated the ERK pathway and increased the activation of ERK in response to TGF-β1. In LMP1-positive cells, treatment with TGF-β1 resulted in more rapid and more robust ERK activation. This increase in ERK activation was maintained through the 72-hour time point. Inhibition of the ERK pathway resulted in protection from TGF-β1–induced EMT. Cells expressing LMP1 and pretreated with the ERK-specific inhibitor, U0126, displayed protection from changes in morphology with TGF-β1 treatment (laboratory observation, data not shown). Pretreatment of LMP1-positive cells with U0126 resulted in complete protection from TGF-β1–induced loss of E-Cad mRNA, and a 95% reduction in the induction of MMP9 mRNA. Inhibition of the ERK pathway reduced, but did not abrogate, the increase in PAI-1, Snail1, and Slug by TGF-β1. These data suggest that, although ERK is a critical pathway for LMP1 and TGF-β1 to induce EMT in human lung epithelial cells, there are multiple pathways with varying contributions to EMT induction.

A novel finding of our work is that the LMP1-mediated reduction of TGF-β1–induced Smad activation is attributable to the reduction in cPML and consequent disruption of the SARA–cPML–Smad activation complex. In this complex, cPML acts as a linking protein, and has been shown to be essential to activation of Smad by TGF-β1 (19). The reduction in cPML reduces the association of cPML and SARA, and the resultant activation of Smad. Although TGF-β1–induced phosphorylation of Smad is reduced with LMP1 expression, the levels remained above that of cells not treated with TGF-β1. The Smad-dependent TGF-β1 up-regulation of PAI-1 is involved in TGFβ-1–induced EMT and the progression of IPF, and was unaffected (HPL1D) or enhanced (A549) by the expression of LMP1, indicating that the Smad pathway remained at least partially activated.

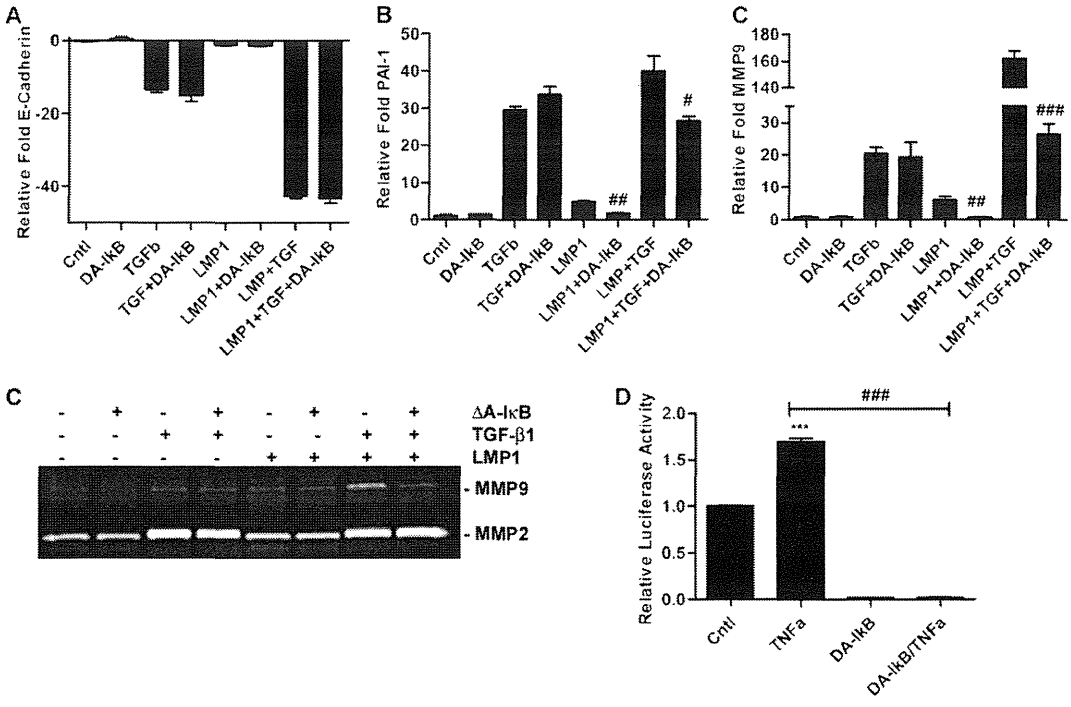

Figure 7. LMP1 pro-EMT signaling is through the nuclear factor (NF)–κB pathway. (*A*–*C*) Real-time qRT-PCR of MMP9, E-Cad, and PAI-1 mRNA expression levels 24 hours after transfection and cotreatment with 1 ng/ml TGF-β1. (*D*) Gelatin zymography detecting MMP2 and -9 in conditioned medium obtained 24 hours after transfection and cotreatment with 1 ng/ml TGF-β1. (*E*) DA-IkB construct and NF-κB–responsive reporter construct were cotransfected in A549 cells. Luciferase activity was assessed 29 hours after transfection (5 hr after treatment with 10 ng/ml TNF-α). $^{***}P < 0.001$ compared with control; $^{\#}P < 0.05$ inhibitor compared with condition without inhibitor; $^{\#\#}P < 0.01$ inhibitor compared with condition without inhibitor; $^{\#\#\#}P < 0.001$ inhibitor compared with condition without inhibitor.

Hypermethylation of the E-Cad (CDH1) gene promoter has been proposed as the mechanism by which LMP1 suppresses E-Cad (36). Treatment with TGF-β1 promoted the loss of E-Cad through transcriptional regulation, whereas LMP1 reduced E-Cad expression at the protein level only. However, the TGF-β1–induced suppression of E-Cad transcription more than doubled when LMP1 was present. Both the TGF-β1–induced suppression of E-Cad transcription and the LMP1 regulation of E-Cad protein were found to be ERK dependent, as demonstrated by experiments employing U0126. Thus, for this marker of EMT, two separate mechanisms dependent on a central signaling pathway were involved. Although the mechanism of E-Cad suppression at the protein level by LMP1 was inconsequential, under cotreatment conditions LMP1 primes the cells for the TGF-β1 response.

MMP9 is up-regulated in cells undergoing EMT (37). Moreover, elevated MMP9 expression has been implicated in the pathogenesis of IPF (38), and is associated with a poorer prognosis (39). Activation of the ERK pathway has been implicated in LMP1-induced up-regulation of MMP9 (40), and analysis of the MMP9 promoter region has shown two active AP1 sites and one active NF-κB site (41). Inhibition of NF-κB eliminated the LMP1 component, but had no affect on TGF-β1 induction of MMP9 at the transcription level; blocking NF-κB reduced the cotreatment induction to that of TGF-β1 treatment alone. Similarly, inhibition of ERK activation abrogated TGF-β1 induction of MMP9, but had little effect on the LMP1 induction of MMP9 transcription. The mechanism of MMP9 up-regulation by LMP1 and TGF-β1 displays two separate signaling pathways converging at the promoter region of the MMP9 gene to increase transcription synergistically. The significance of this finding is that MMP9 preferentially degrades type IV collagen, a major component of the basement membrane, and, in turn, disruption of the basement membrane is permissive for fibrogenesis. Thus, the synergistic up-regulation of MMP9 by TGF-β1 in LMP1-positive cells may be a mechanism by which latent EBV infection exacerbates fibrogenesis.

Attempts to characterize the LMP1 and TGF-β1 synergy in mouse (C10, MLE12) and rat (RLE12) lung epithelial cells were unsuccessful, and, unfortunately, preclude our ability to look at LMP-1 and TGF-β1 in a murine model of lung fibrosis. Although LMP1 was expressed in cells transiently transfected, retrovirally transduced, or infected by LMP1 adenovirus expression vectors in murine cells, the proteomics explored were essentially unchanged when compared with the control vector. More significant to this study, the response to TGF-β1 by LMP1-positive mouse or rat lung epithelial cells was not significantly different from the TGF-β1 response of parental control cells. This species-specific phenomenon is consistent with the genetics of the EBV in comparison to the murid herpes virus (MHV) 4. Although MHV4 has been used as a model for γ-Herpeviridae infection of the lung, this virus does not encode a protein homologous to LMP1 (42). Thus, MHV4 can be used as a tool for studying the deleterious effects of lytic herpes viral replication and subsequent cellular damage in lung epithelium, but not for studying the molecular mechanisms of latent EBV infection of the lung. The lack of an LMP1 homolog suggests differential signaling in mouse verses human epithelium. Although expression of LMP1 in transgenic mouse lines targeted to the B cells promotes lymphomas (43) and mimics CD40 signaling (44), similar to the expression seen in humans, expression of LMP1 in murine pulmonary epithelial cells is not analogous to the signaling characteristics of LMP1 expression in human lung epithelial cells, and does not provide an appropriate model for this study.

The pathology of usual interstitial pneumonia in IPF has been well characterized, although the exact molecular mechanisms are proving to be more elusive. This study provides evidence for a model of disease progression attributable to viral influences. As a consequence of EBV in the lung epithelium and expression of LMP1, the cells are primed for exuberant expression and activation of MMP9, as well as for a pro-EMT response to TGF-β1. This synergistic overall effect is independent of the TGF-β1–mediated up-regulation of Snail and Slug;

however, the majority of the pro-EMT effects are cooperative. The up-regulation of PAI-1, N-Cad, aSMA, collagen 1, and vimentin by TGF-β1 and LMP1 is additive, whereas the up-regulation of MMP9 and loss of E-Cad are synergistic. The net effect on treatment of lung epithelial cells expressing LMP1 with low-dose TGF-β1 is an augmentation of EMT.

Author Disclosure: E.K.F. received sponsored grants from the National Institutes of Health (NIH) for $1,001–$5,000 and more than $100,001; J.A.L. served on the Data Safety Monitoring Board for Boehringer Ingelheim, Actelion, and Centocor for $1,001–$5,000 each, and sponsored grants from NIH and InterMune for $50,001–$100,000 each, and Novartis for more than $100,001; T.T. serves on the advisory board of Oncomics for up to $1,000, and has received lecture fees from Merck Banyu and Fuji Film for up to $1,000 each, royalties from Oncomics for $1,001–$5,000, owns stock for $10,001–$50,000, and received a sponsored grant from Ministry of Education, Culture, Sports, Science and Technology (Japanese government) for more than $100,001 and from the Smoking Research Foundation for $50,001–$100,000; none of the other authors has a financial relationship with a commercial entity that has an interest in the subject of this manuscript.

References

1. American Thoracic Society. Idiopathic pulmonary fibrosis: diagnosis and treatment. International consensus statement. American Thoracic Society (ATS), and the European Respiratory Society (ERS). *Am J Respir Crit Care Med* 2000;161:646–664.
2. Mora AL, Torres-Gonzalez E, Rojas M, Xu J, Ritzenthaler J, Speck SH, Roman J, Brigham K, Stecenko A. Control of virus reactivation arrests pulmonary herpesvirus-induced fibrosis in IFN-gamma receptor-deficient mice. *Am J Respir Crit Care Med* 2007;175:1139–1150.
3. Selman M, King TE, Pardo A. Idiopathic pulmonary fibrosis: prevailing and evolving hypotheses about its pathogenesis and implications for therapy. *Ann Intern Med* 2001;134:136–151.
4. Vergnon JM, Vincent M, de The G, Mornex JF, Weynants P, Brune J. Cryptogenic fibrosing alveolitis and Epstein-Barr virus: an association? *Lancet* 1984;2:768–771.
5. Egan JJ, Stewart JP, Hasleton PS, Arrand JR, Carroll KB, Woodcock AA. Epstein-Barr virus replication within pulmonary epithelial cells in cryptogenic fibrosing alveolitis. *Thorax* 1995;50:1234–1239.
6. Stewart JP, Egan JJ, Ross AJ, Kelly BG, Lok SS, Hasleton PS, Woodcock AA. The detection of Epstein-Barr virus DNA in lung tissue from patients with idiopathic pulmonary fibrosis. *Am J Respir Crit Care Med* 1999;159:1336–1341.
7. Tang YW, Johnson JE, Browning PJ, Cruz-Gervis RA, Davis A, Graham BS, Brigham KL, Oates JA, Jr., Loyd JE, Stecenko AA. Herpesvirus DNA is consistently detected in lungs of patients with idiopathic pulmonary fibrosis. *J Clin Microbiol* 2003;41:2633–2640.
8. Tsukamoto K, Hayakawa H, Sato A, Chida K, Nakamura H, Miura K. Involvement of Epstein-Barr virus latent membrane protein 1 in disease progression in patients with idiopathic pulmonary fibrosis. *Thorax* 2000;55:958–961.
9. Yonemaru M, Kasuga I, Kusumoto H, Kunisawa A, Kiyokawa H, Kuwabara S, Ichinose Y, Toyama K. Elevation of antibodies to cytomegalovirus and other herpes viruses in pulmonary fibrosis. *Eur Respir J* 1997;10:2040–2045.
10. Eliopoulos AG, Young LS. LMP1 structure and signal transduction. *Semin Cancer Biol* 2001;11:435–444.
11. Dawson CW, Laverick L, Morris MA, Tramoutanis G, Young LS. Epstein-Barr virus–encoded LMP1 regulates epithelial cell motility and invasion via the ERK–MAPK pathway. *J Virol* 2008;82:3654–3664.
12. Dawson CW, Rickinson AB, Young LS. Epstein-Barr virus latent membrane protein inhibits human epithelial cell differentiation. *Nature* 1990;344:777–780.
13. Dawson CW, Tramountanis G, Eliopoulos AG, Young LS. Epstein-Barr virus latent membrane protein 1 (LMP1) activates the phosphatidylinositol 3-kinase/Akt pathway to promote cell survival and induce actin filament remodeling. *J Biol Chem* 2003;278:3694–3704.
14. Horikawa T, Yang J, Kondo S, Yoshizaki T, Joab I, Furukawa M, Pagano JS. Twist and epithelial–mesenchymal transition are induced by the EBV oncoprotein latent membrane protein 1 and are associated with metastatic nasopharyngeal carcinoma. *Cancer Res* 2007;67:1970–1978.
15. Thiery JP, Sleeman JP. Complex networks orchestrate epithelial–mesenchymal transitions. *Nat Rev Mol Cell Biol* 2006;7:131–142.
16. Kim KK, Kugler MC, Wolters PJ, Robillard L, Galvez MG, Brumwell AN, Sheppard D, Chapman HA. Alveolar epithelial cell mesenchymal transition develops *in vivo* during pulmonary fibrosis and is regulated by the extracellular matrix. *Proc Natl Acad Sci USA* 2006;103:13180–13185.
17. Willis BC, duBois RM, Borok Z. Epithelial origin of myofibroblasts during fibrosis in the lung. *Proc Am Thorac Soc* 2006;3:377–382.
18. Letterio JJ, Roberts AB. Regulation of immune responses by TGF-beta. *Annu Rev Immunol* 1998;16:137–161.
19. Lin HK, Bergmann S, Pandolfi PP. Cytoplasmic PML function in TGF-beta signalling. *Nature* 2004;431:205–211.
20. Shi Y, Massague J. Mechanisms of TGF-beta signaling from cell membrane to the nucleus. *Cell* 2003;113:685–700.
21. Willis BC, Borok Z. TGF-beta–induced EMT: mechanisms and implications for fibrotic lung disease. *Am J Physiol Lung Cell Mol Physiol* 2007;293:L525–L534.
22. Kasai H, Allen JT, Mason RM, Kamimura T, Zhang Z. TGF-beta1 induces human alveolar epithelial to mesenchymal cell transition (EMT). *Respir Res* 2005;6:56.
23. Malizia AP, Keating DT, Smith SM, Walls D, Doran PP, Egan JJ. Alveolar epithelial cell injury with Epstein-Barr virus upregulates TGFbeta1 expression. *Am J Physiol Lung Cell Mol Physiol* 2008;295:L451–L460.
24. Masuda A, Kondo M, Saito T, Yatabe Y, Kobayashi T, Okamoto M, Suyama M, Takahashi T. Establishment of human peripheral lung epithelial cell lines (HPL1) retaining differentiated characteristics and responsiveness to epidermal growth factor, hepatocyte growth factor, and transforming growth factor beta1. *Cancer Res* 1997;57:4898–4904.
25. Shan B, Yao TP, Nguyen HT, Zhuo Y, Levy DR, Klingsberg RC, Tao H, Palmer ML, Holder KN, Lasky JA. Requirement of HDAC6 for transforming growth factor–beta1–induced epithelial–mesenchymal transition. *J Biol Chem* 2008;283:21065–21073.
26. Cameron JE, Yin Q, Fewell C, Lacey M, McBride J, Wang X, Lin Z, Schaefer BC, Flemington EK. Epstein-Barr virus latent membrane protein 1 induces cellular MicroRNA miR-146a, a modulator of lymphocyte signaling pathways. *J Virol* 2008;82:1946–1958.
27. Brockman JA, Scherer DC, McKinsey TA, Hall SM, Qi X, Lee WY, Ballard DW. Coupling of a signal response domain in I kappa B alpha to multiple pathways for NF-kappa B activation. *Mol Cell Biol* 1995;15:2809–2818.
28. Gottschalk S, Edwards OL, Sili U, Huls MH, Goltsova T, Davis AR, Heslop HE, Rooney CM. Generating CTLs against the subdominant Epstein-Barr virus LMP1 antigen for the adoptive immunotherapy of EBV-associated malignancies. *Blood* 2003;101:1905–1912.
29. Yue X, Li X, Nguyen HT, Chin DR, Sullivan DE, Lasky JA. Transforming growth factor–beta1 induces heparan sulfate 6-O-endosulfatase 1 expression *in vitro* and *in vivo*. *J Biol Chem* 2008;283:20397–20407.
30. Yang L, Amann JM, Kikuchi T, Porta R, Guix M, Gonzalez A, Park KH, Billheimer D, Arteaga CL, Tai HH, *et al.* Inhibition of epidermal growth factor receptor signaling elevates 15-hydroxyprostaglandin dehydrogenase in non–small-cell lung cancer. *Cancer Res* 2007;67:5587–5593.
31. Molesworth SJ, Lake CM, Borza CM, Turk SM, Hutt-Fletcher LM. Epstein-Barr virus gH is essential for penetration of B cells but also plays a role in attachment of virus to epithelial cells. *J Virol* 2000;74:6324–6332.
32. Shan B, Zhuo Y, Chin D, Morris CA, Morris GF, Lasky JA. Cyclin-dependent kinase 9 is required for tumor necrosis factor–alpha–stimulated matrix metalloproteinase–9 expression in human lung adenocarcinoma cells. *J Biol Chem* 2005;280:1103–1111.
33. Vannella KM, Luckhardt TR, Wilke CA, van Dyk LF, Toews GB, Moore BB. Latent herpesvirus infection augments experimental pulmonary fibrosis. *Am J Respir Crit Care Med* 2010;181:465–477.
34. Ranganathan P, Agrawal A, Bhushan R, Chavalmane AK, Kalathur RK, Takahashi T, Kondaiah P. Expression profiling of genes regulated by TGF-beta: differential regulation in normal and tumour cells. *BMC Genomics* 2007;8:98.
35. Xie L, Law BK, Chytil AM, Brown KA, Aakre ME, Moses HL. Activation of the Erk pathway is required for TGF-beta1–induced EMT in vitro. *Neoplasia* 2004;6:603–610.
36. Tsai CN, Tsai CL, Tse KP, Chang HY, Chang YS. The Epstein-Barr virus oncogene product, latent membrane protein 1, induces the down-regulation of E-cadherin gene expression via activation of DNA methyltransferases. *Proc Natl Acad Sci USA* 2002;99:10084–10089.
37. Tester AM, Ruangpanit N, Anderson RL, Thompson EW. MMP-9 secretion and MMP-2 activation distinguish invasive and metastatic

sublines of a mouse mammary carcinoma system showing epithelial–mesenchymal transition traits. *Clin Exp Metastasis* 2000; 18:553–560.
38. Suga M, Iyonaga K, Okamoto T, Gushima Y, Miyakawa H, Akaike T, Ando M. Characteristic elevation of matrix metalloproteinase activity in idiopathic interstitial pneumonias. *Am J Respir Crit Care Med* 2000;162:1949–1956.
39. McKeown S, Richter AG, O'Kane C, McAuley DF, Thickett DR. MMP expression and abnormal lung permeability are important determinants of outcome in IPF. *Eur Respir J* 2009;33:77–84.
40. Liu LT, Peng JP, Chang HC, Hung WC. RECK is a target of Epstein-Barr virus latent membrane protein 1. *Oncogene* 2003;22:8263–8270.
41. Yan C, Boyd DD. Regulation of matrix metalloproteinase gene expression. *J Cell Physiol* 2007;211:19–26.
42. Virgin HWt, Latreille P, Wamsley P, Hallsworth K, Weck KE, Dal Canto AJ, Speck SH. Complete sequence and genomic analysis of murine gammaherpesvirus 68. *J Virol* 1997;71:5894–5904.
43. Kulwichit W, Edwards RH, Davenport EM, Baskar JF, Godfrey V, Raab-Traub N. Expression of the Epstein-Barr virus latent membrane protein 1 induces B cell lymphoma in transgenic mice. *Proc Natl Acad Sci USA* 1998;95:11963–11968.
44. Panagopoulos D, Victoratos P, Alexiou M, Kollias G, Mosialos G. Comparative analysis of signal transduction by CD40 and the Epstein-Barr virus oncoprotein LMP1 *in vivo*. *J Virol* 2004;78:13253–13261.

0022-3565/11/3362-551–559$20.00
THE JOURNAL OF PHARMACOLOGY AND EXPERIMENTAL THERAPEUTICS
JPET 336:551–559, 2011

Vol. 336, No. 2
173120/3661988
Printed in U.S.A.

Mechanisms of Amiodarone and Desethylamiodarone Cytotoxicity in Nontransformed Human Peripheral Lung Epithelial Cells

Jeanne E. Mulder, James F. Brien, William J. Racz, Takashi Takahashi, and Thomas E. Massey

Department of Pharmacology and Toxicology, Queen's University, Kingston, Ontario, Canada (J.E.M., J.F.B., W.J.R., T.E.M.); and Division of Molecular Carcinogenesis, Center for Neurological Diseases and Cancer, Nagoya University Graduate School of Medicine, Nagoya, Japan (T.T.)

Received July 19, 2010; accepted November 11, 2010

ABSTRACT

Amiodarone (AM) is a potent antidysrhythmic agent that can cause potentially life-threatening pulmonary fibrosis, and *N*-desethylamiodarone (DEA), an AM metabolite, may contribute to AM toxicity. Apoptotic cell death in nontransformed human peripheral lung epithelial 1A (HPL1A) cells was assessed by annexin V-fluorescein isothiocyanate (ann-V) staining and terminal deoxynucleotidyl transferase-mediated dUTP nick-end labeling (TUNEL), and necrotic cell death was assessed by propidium iodide (PI) staining. The percentage of cells that were PI-positive increased more than six times with 20 μM AM and approximately doubled with 3.5 μM DEA, relative to control. The percentage of cells that were ann-V-positive decreased by more than 80% after 24-h exposure to 10 μM AM but more than doubled after 24-h incubation with 3.5 μM DEA. Incubation for 24 h with 5.0 μM DEA increased the percentage of cells that were TUNEL-positive more than six times. Incubation with AM (2.5 μM) or DEA (1–2 μM) for 24 h did not significantly alter angiotensinogen mRNA levels. Furthermore, angiotensin II (100 pM–1 μM) alone or in combination with AM or DEA did not alter cytotoxicity, and pretreatment with the angiotensin-converting enzyme inhibitor and antioxidant captopril (3–6 μM) did not protect against AM or DEA cytotoxicity. In conclusion, AM activates primarily necrotic pathways, whereas DEA activates both necrotic and apoptotic pathways, and the renin-angiotensin system does not seem to be involved in AM or DEA cytotoxicity in HPL1A cells.

Introduction

Amiodarone (AM), an iodinated benzofuran, is considered to be the most efficacious antidysrhythmic drug currently available (Lafuente-Lafuente et al., 2009). However, long-term treatment with AM is associated with several adverse effects, the one of greatest concern being AM-induced pulmonary toxicity (AIPT), because it can progress to potentially life-threatening pulmonary fibrosis. Recent studies have reported that the incidence of AIPT occurs in 5 to 13% of patients treated with AM in a dose- and duration-dependent manner (Oyama et al., 2005). The prognosis of a patient with AIPT is poor, with a 10 to 23% mortality rate (Vrobel et al., 1989; Oyama et al., 2005).

AM and its major pharmacological active metabolite, desethylamiodarone (DEA), have large apparent volumes of distribution and slow clearances from adipose tissue, liver, lungs, and lymph nodes and therefore accumulate to high concentrations in these tissues (Freedman and Somberg, 1991). After long-term therapy, AM can accumulate in lung to >1 mmol/kg wet tissue (Brien et al., 1987). In addition, DEA has greater cytotoxic potency than AM and can accumulate in lung to up to four times greater levels than AM (Broekhuysen et al., 1969; Wilson and Lippmann, 1990; Reasor and Kacew, 1996). Hence, there is compelling evidence that DEA plays a role in AIPT.

The underlying etiology of AIPT is unknown; however, both indirect inflammatory processes and direct toxic effects have been proposed previously (Reasor and Kacew, 1996). AM and DEA are directly toxic to bovine arterial endothelial

This work was supported by the Canadian Institutes of Health Research [Grant MOP-13257].
Article, publication date, and citation information can be found at http://jpet.aspetjournals.org.
doi:10.1124/jpet.110.173120.

ABBREVIATIONS: AM, amiodarone; AIPT, AM-induced pulmonary toxicity; DEA, desethylamiodarone; RAS, renin-angiotensin system; Ang II, angiotensin II; ann-V, annexin-V-fluorescein isothiocyanate; AGTR, angiotensin receptor; PI, propidium iodide; HPL1A, human peripheral lung epithelial cells; PCR, polymerase chain reaction; TUNEL, terminal deoxynucleotidyl transferase-mediated dUTP nick-end labeling; PBS, phosphate-buffered saline; HPLC, high-performance liquid chromatography; ANOVA, analysis of variance.

cells, alveolar macrophages, interstitial lung fibroblasts (Martin and Howard, 1985), human pulmonary arterial endothelial cells (Powis et al., 1990), bronchial epithelial cells (Colgan et al., 1984), and hepatocytes (Gross et al., 1989). Many mechanisms have been hypothesized to cause the direct toxicity of AM and DEA, including increased intracellular influx of Ca^{2+} (Powis et al., 1990), mitochondrial disruption (Bolt et al., 2001), free radical and reactive oxygen species formation (Pollak, 1999), and up-regulation of the renin-angiotensin system (RAS) (Uhal et al., 2007).

Studies have indicated that rat lung epithelial cells and human lung adenocarcinoma cells have an intrinsic RAS, with the ability to generate angiotensin II (Ang II) de novo (Li et al., 2003). Ang II signaling, mediated via the angiotensin receptors AGTR1 and AGTR2, plays a role in tissue remodeling in fibrosis (Königshoff et al., 2007). However, the downstream effects of AGTR1 and AGTR2 activation are quite different. The classic physiologic effects of Ang II, including vasoconstriction, aldosterone and vasopressin release, sodium and water retention, and cell proliferation, are mediated by AGTR1, whereas the established role of AGTR2 includes modulation of biological processes involved in development, cell differentiation, tissue repair, and apoptosis (Kaschina and Unger, 2003). Ang II can induce concentration-dependent apoptosis in human lung cancer epithelial cells and in primary type II pneumocytes isolated from adult Wistar rats, an effect that can be abrogated by the nonselective AGTR antagonist saralasin (Wang et al., 1999b). In addition, treatment with the angiotensin-converting enzyme inhibitor captopril can attenuate apoptosis in human lung adenocarcinoma cells and primary rat alveolar epithelial cells treated with AM or DEA (Bargout et al., 2000) and can inhibit alveolar wall collagen formation in lungs of AM-treated rats (Uhal et al., 2003). Furthermore, a retrospective review of patients taking AM suggests that patients who developed AIPT were administered a lower dose of RAS inhibitor than those who did not develop AIPT (Nikaido et al., 2008). Thus, the RAS may play a contributing role in the initiation and/or progression of AIPT.

Surfactant-secreting type II alveolar epithelial cells provide antioxidant defense, local immunomodulation, and a stem cell reserve for alveolar epithelial repair and are critical for normal re-epithelialization and healing without fibrosis of the alveolar surface (Thannickal et al., 2004). Histological analysis of lung tissue from patients treated with AM demonstrates alveolar interstitial damage, including hyperplasia of type II pneumocytes (Brien et al., 1987). In addition, AM is toxic to epithelial cells in vitro (Bargout et al., 2000), thereby implicating epithelial injury in the initiation of AIPT. To better understand the etiology of AIPT, the present study investigated the cytotoxic pathways activated by AM or DEA individually and whether an intrinsic RAS is linked to AM- or DEA-induced cell death. HPL1A cells, which were established by immortalization from a normal adult lung specimen, were employed because they retain morphological and biochemical features characteristic of normal adult human peripheral lung epithelial cells (Masuda et al., 1997).

Materials and Methods

Reagents. Chemicals and reagents were obtained as follows: AM HCl (98% purity), bovine insulin, fetal bovine serum, hydrocortisone, HEPES, Ang II, captopril, propidium iodide (PI), and trypan blue from Sigma-Aldrich (Oakville, ON, Canada); annexin V-fluorescein isothiocyanate (ann-V) from BD Biosciences (Mississauga, ON, Canada); glacial acetic acid, KH_2PO_4, NaCl, $NaHCO_3$, NaOH, and $Na_2HPO_4{\cdot}7H_2O$ from Thermo Fisher Scientific (Nepean, ON, Canada); and antibiotic-antimycotic, L-glutamine, Ham's F-12 nutrient mixture, human transferrin, and trypsin-EDTA from Invitrogen Canada Inc. (Burlington, ON, Canada). DEA HCl (99.9% purity) was synthesized by Dr. Manlio Alessi (Department of Chemistry at Queen's University, Kingston, ON). All other reagents were of analytical grade and were purchased from standard commercial suppliers. Stock solutions of 4.0 mM AM, 1.0 mM DEA, 4.8 mM Ang II, and 2.0 mM captopril were prepared fresh in reverse osmosis purified distilled water at 65°C (AM and DEA) or room temperature (Ang II and captopril).

Cell Culture. HPL1A cells (Masuda et al., 1997) were cultured in Ham's F-12 nutrient mixture medium, pH 7.2, supplemented with 1.18 g/liter sodium bicarbonate, 1% fetal bovine serum, 15 mM HEPES buffer, 1× antibiotic-antimycotic, 100 nM hydrocortisone, 0.13 ng/ml triiodothyronine, 5.0 μg/ml human transferrin, and 5.0 μg/ml bovine insulin (HPL1A medium). Cells were grown in T-75 flasks (Corning Inc., Corning, NY). Culture medium was replaced every 3 to 4 days, and cells were subcultured approximately every 7 days between passages 8 and 12. Cells were incubated at 37°C under 95% air, 5% CO_2. After reaching 80 to 90% confluence, cells were removed from tissue culture flasks by washing twice with 10 ml of phosphate-buffered saline (PBS) (0.2 g/liter KH_2PO_4, 0.8 g/liter NaCl, 2.16 g/liter $Na_2HPO_4{\cdot}7H_2O$, pH 7.3), and then treated with 0.1% trypsin and 1.06 mM EDTA in PBS. The cells were then incubated at 37°C for 5 to 10 min and resuspended in HPL1A medium. Cells were seeded at a density of 2.1×10^5 cells/well in 12-well plates or 2.8×10^6 cells/100-mm dish and allowed to acclimatize for approximately 24 h before drug treatment.

Quantification of AM and DEA in HPL1A Cells. To determine whether HPL1A cells are able to convert AM to DEA, the amount of AM and DEA within HPL1A cells after 24 h of treatment was determined by high-performance liquid chromatography (HPLC). In brief, cells in 100-mm dishes were treated with AM for 24 h. Cells were then harvested and centrifuged at 700*g* for 10 min at 4°C. The supernatant was removed, and the cell pellet was resuspended in 1.0 ml of 4°C PBS and then centrifuged at 700*g* for 5 min at 4°C. The supernatant was removed, and the resulting cell pellet was immediately frozen in liquid nitrogen and stored at −80°C until analysis.

The amount of AM and DEA in cell pellets was measured as described by Bolt et al. (1998). In brief, each cell pellet was thawed, and 100 μl of mobile phase [acetonitrile/5% aqueous acetic acid, 8:2 (v/v) adjusted to pH 5.9 with ammonium hydroxide] was added. Cell pellets were mixed in the mobile phase for 1 min, and the mixture was centrifuged at 16,000*g* for 3 min at room temperature. The supernatants were analyzed quantitatively for AM and DEA by reverse-phase HPLC with UV-visible spectrophotometric detection at 254 nm, with a with-in day precision of 7.00% (Brien et al., 1983, 1987). The percentage conversion of AM to DEA for each treatment condition was calculated. The mean value from three independent experiments was used to calculate the overall percent conversion of AM to DEA for each treatment condition. The lower limit of quantifiable detection for DEA was 0.20 μg/ml (0.31 μM). The concentrations of AM and DEA injected onto the HPLC column from biological samples were within the range of standards employed (11.3–180 μg/ml for AM and 0.25–4.00 μg/ml for DEA).

Annexin-V-Fluorescein Isothiocyanate and Propidium Iodide Dual Staining. HPL1A cells were stained with ann-V to indicate apoptosis and PI to indicate necrosis. For AM and DEA cytotoxicity experiments, HPL1A cells in 12-well plates were treated with AM or DEA for 6, 12, or 24 h. For Ang II cytotoxicity experiments, HPL1A cells in 12-well plates were treated with AM or DEA in combination with Ang II for 24 h. Ang II was administered every 12 h in the 24-h treatment period. For captopril protection experiments,